Radiation Effects in Silicon Photonics Micro-Ring Modulators and Waveguides for High-Energy Physics

Daniele Alfiero

Seminar

University of Birmingham

daniele.alfiero@cern.ch | 28.05.2026

CERN

UNIVERSITY OF BIRMINGHAM

Outline

- **Introduction**
  - Silicon Photonics for high-speed links in particle detectors
  - Ring modulators and waveguides
- **Irradiation campaigns**
  - X-ray test on ring modulators:
    - Electro-optic frequency response
    - Localized thermal annealing
  - Neutron and X-ray tests on waveguides:
    - Radiation-induced attenuation (RIA)
  - Heavy ion test on waveguides:
    - Optical single-event transients (OSETs)
    - TCAD simulations
- **Conclusions and future work**

Introduction

Silicon Photonics for High-Energy Physics

Introduction – Silicon Photonics for High-Energy Physics

Silicon Photonics

- ✓ High-speed data transmission
- ✓ Low mass
- ✓ Low power consumption
- ✓ CMOS compatible process flow
- ? Radiation hardness

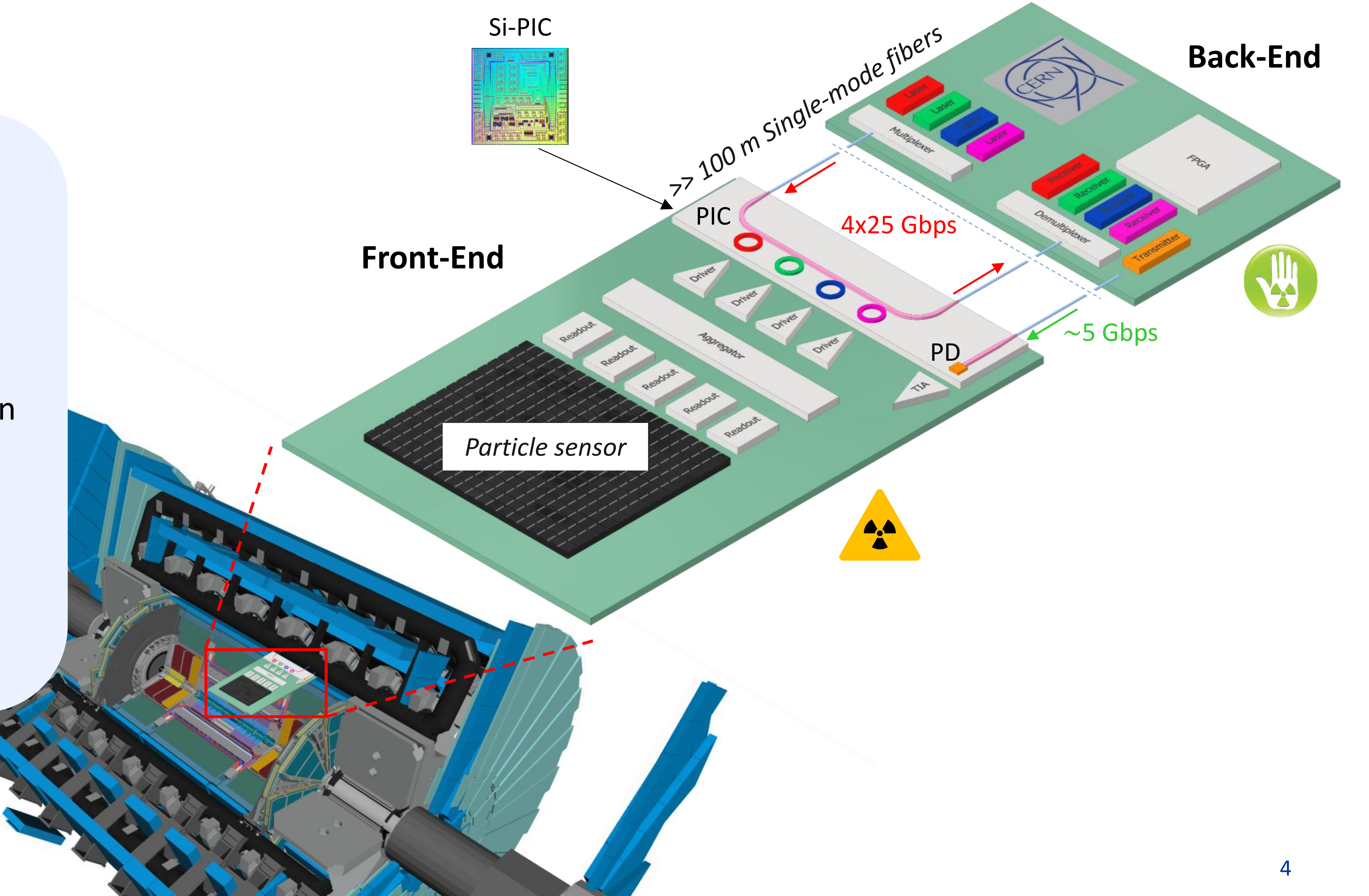

PIC: Photonic Integrated Circuit
PD: Photodiode

Introduction – Overview of a SiPh-based transceiver

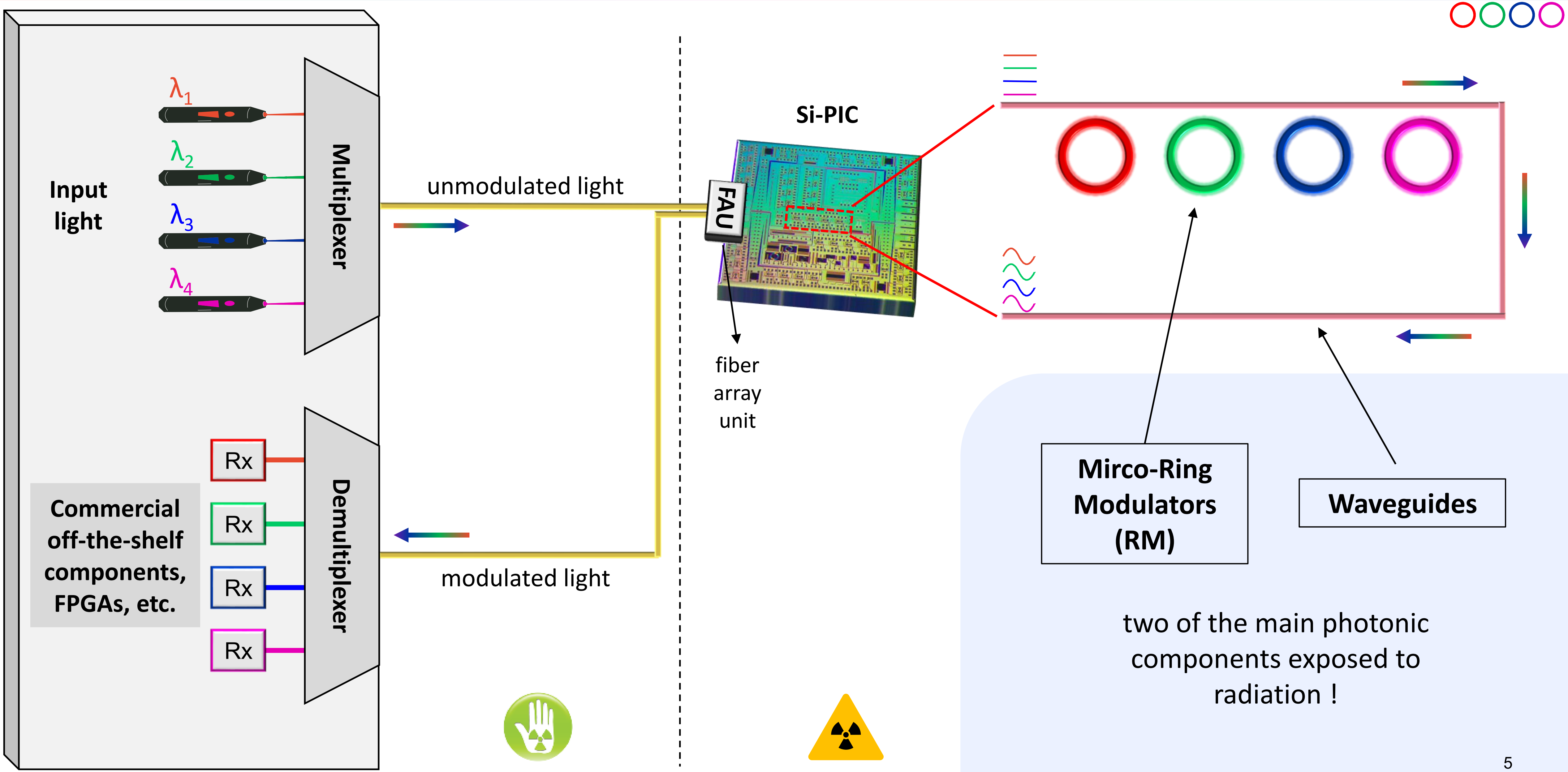

two of the main photonic components exposed to radiation !

Introduction – Light coupling and waveguides

Edge coupler

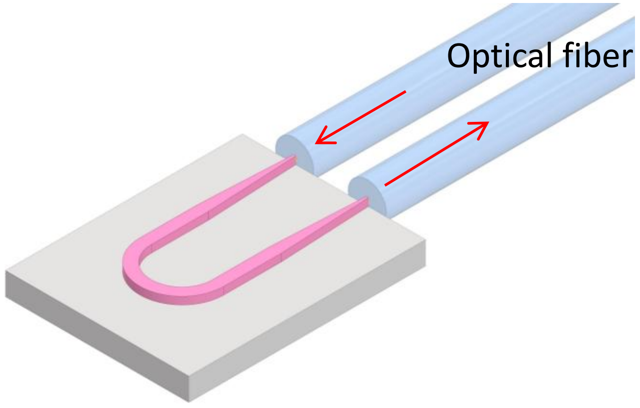

Vertical coupler

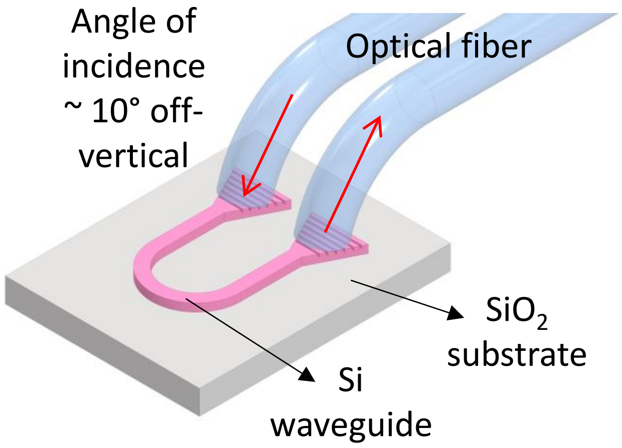

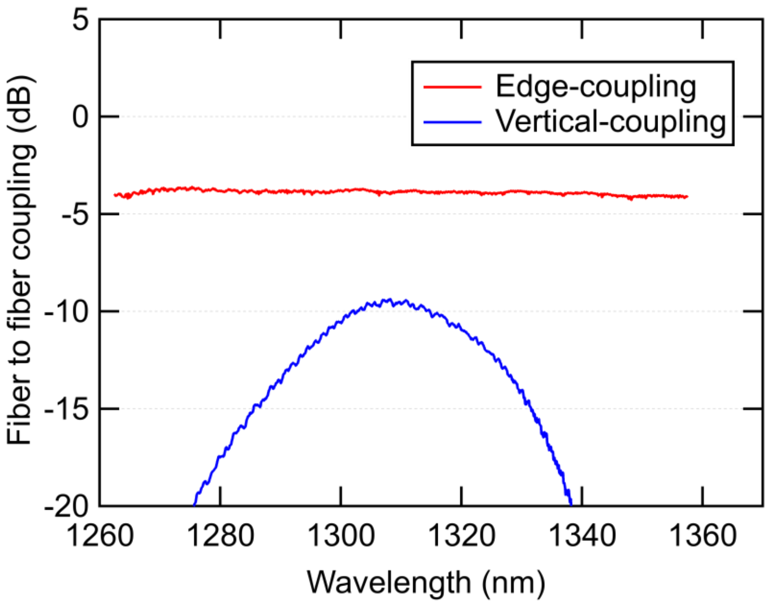

	Edge	Vertical
Insertion Loss	✓	✗
Bandwidth	✓	✗
Packaging Complexity	O	✓
Wafer Level Probing	O	✓

Waveguides cross-section

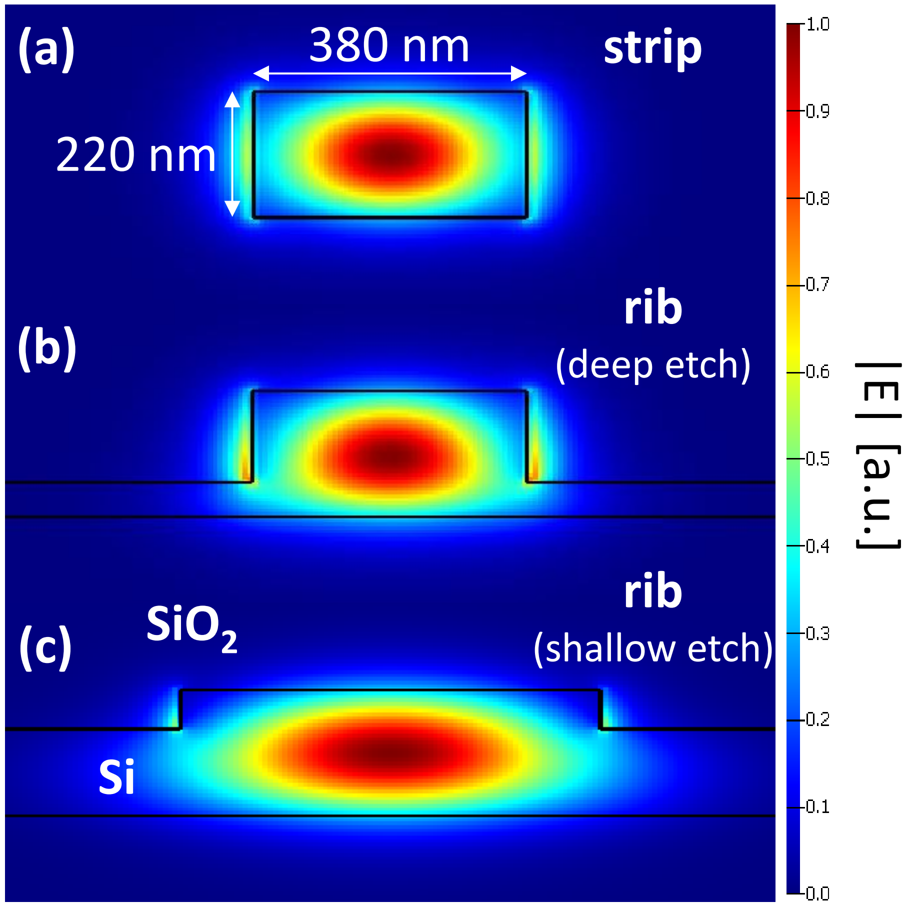

Introduction – Ring Modulators

Working principle:

- Light coupled into the silicon micro-ring
- Destructive interference → **resonance**

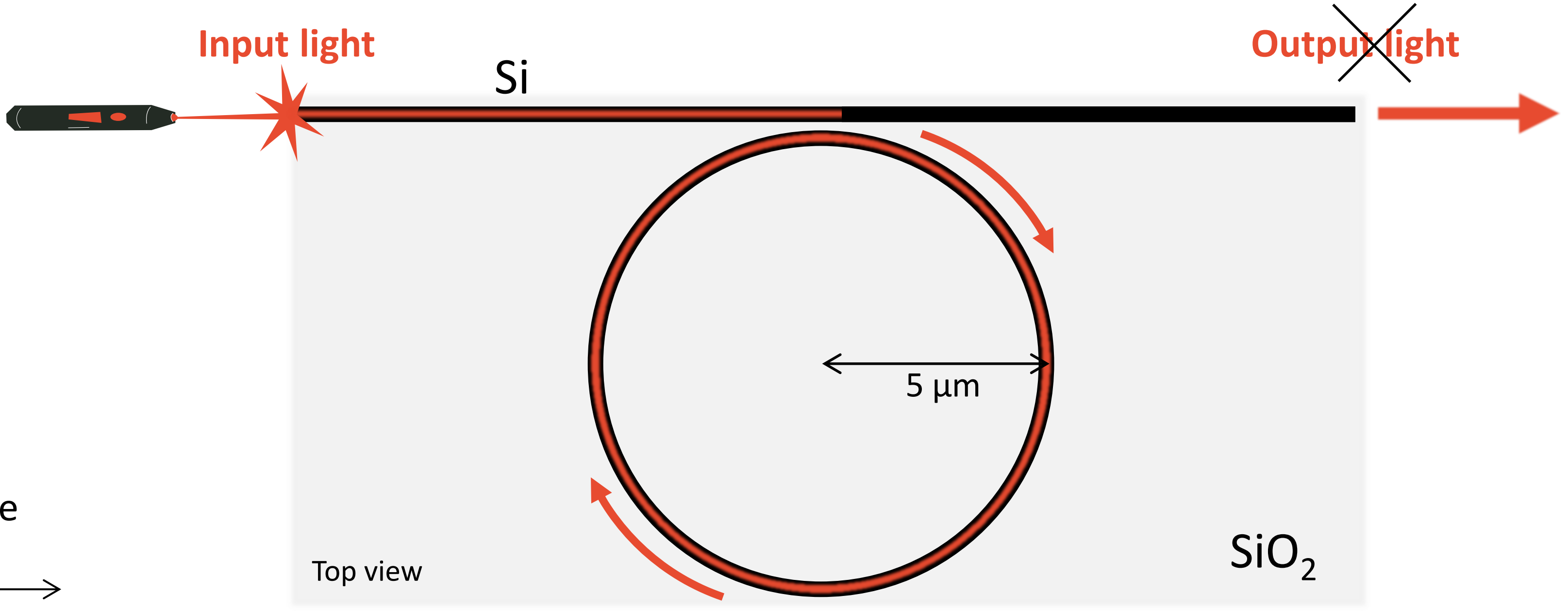

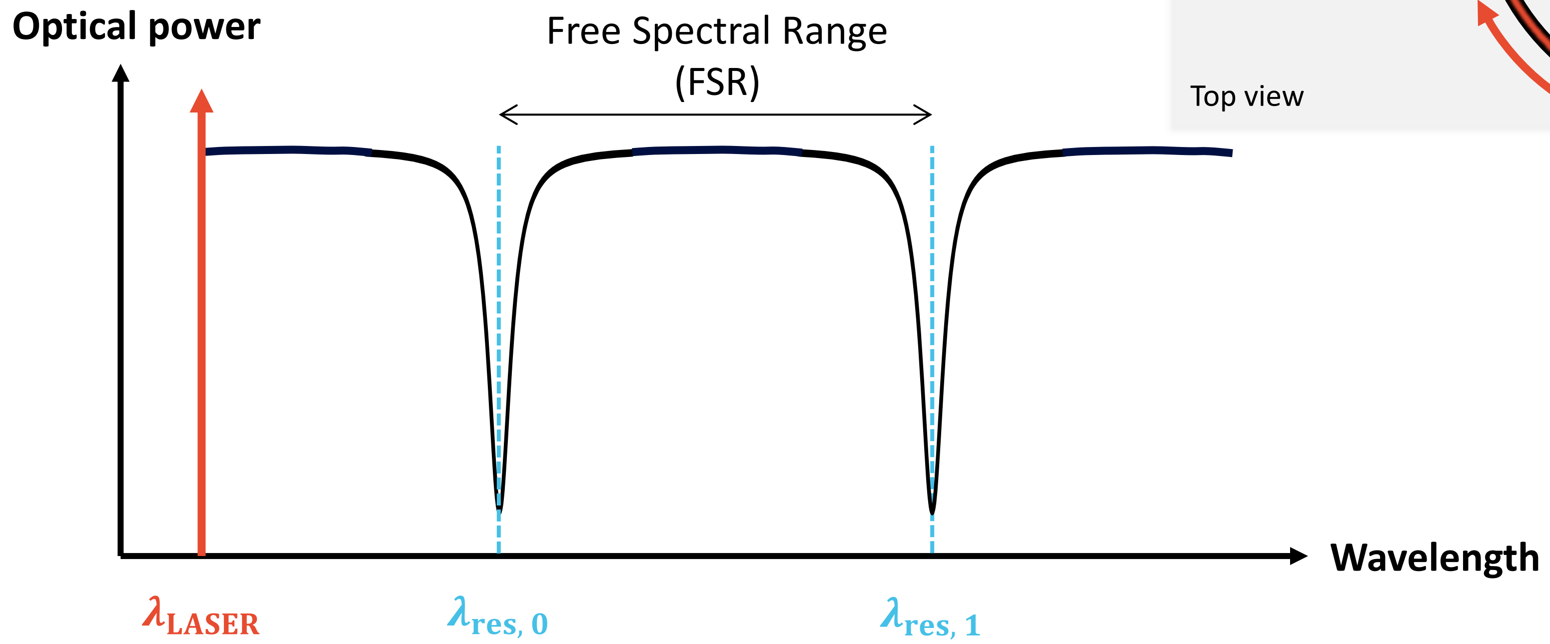

$$\lambda_{\mathrm{res},\,m} = \frac{n_{\mathrm{eff}} L}{m}, \qquad m = 1, 2, 3, \ldots$$

n_{eff}: effective refractive index
L: round trip length

How do we modulate it?

- Modulation of the resonance peak through the applied voltage
  - **Injection/depletion of carriers** → variation of the effective refractive index

$$\Delta n \propto -(\Delta N_{\text{electrons}} + \Delta N_{\text{holes}})$$

$$\Delta \alpha \propto (\Delta N_{\text{electrons}} + \Delta N_{\text{holes}})$$

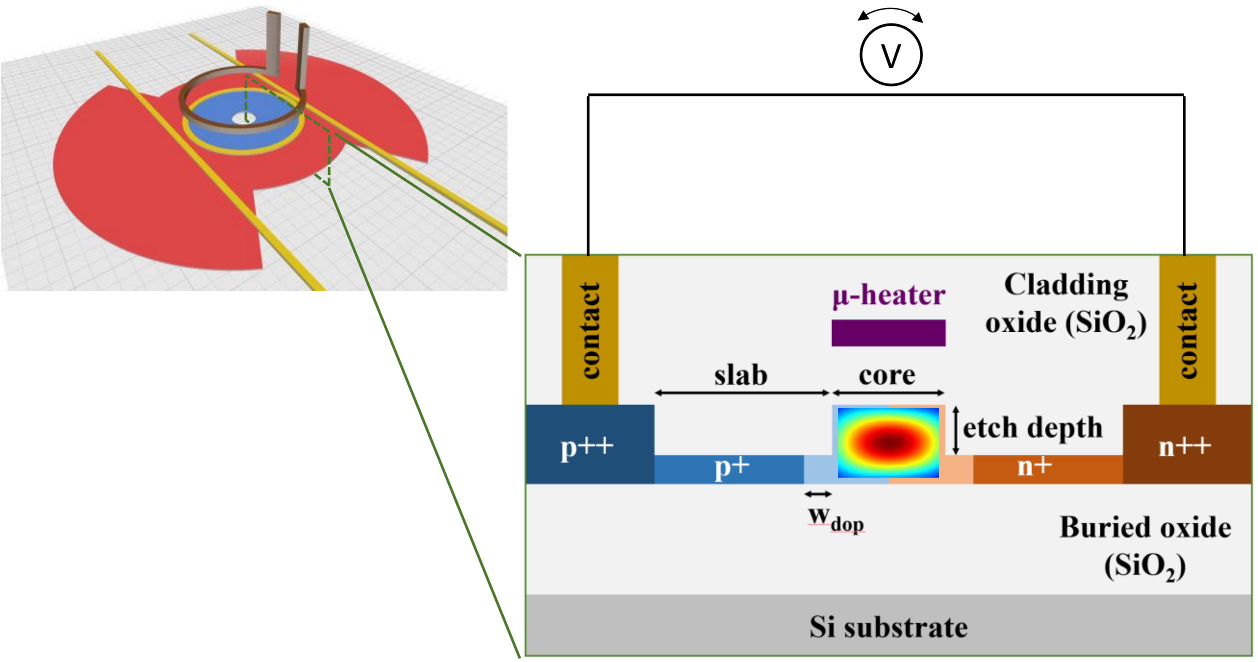

Phase shifter cross-section

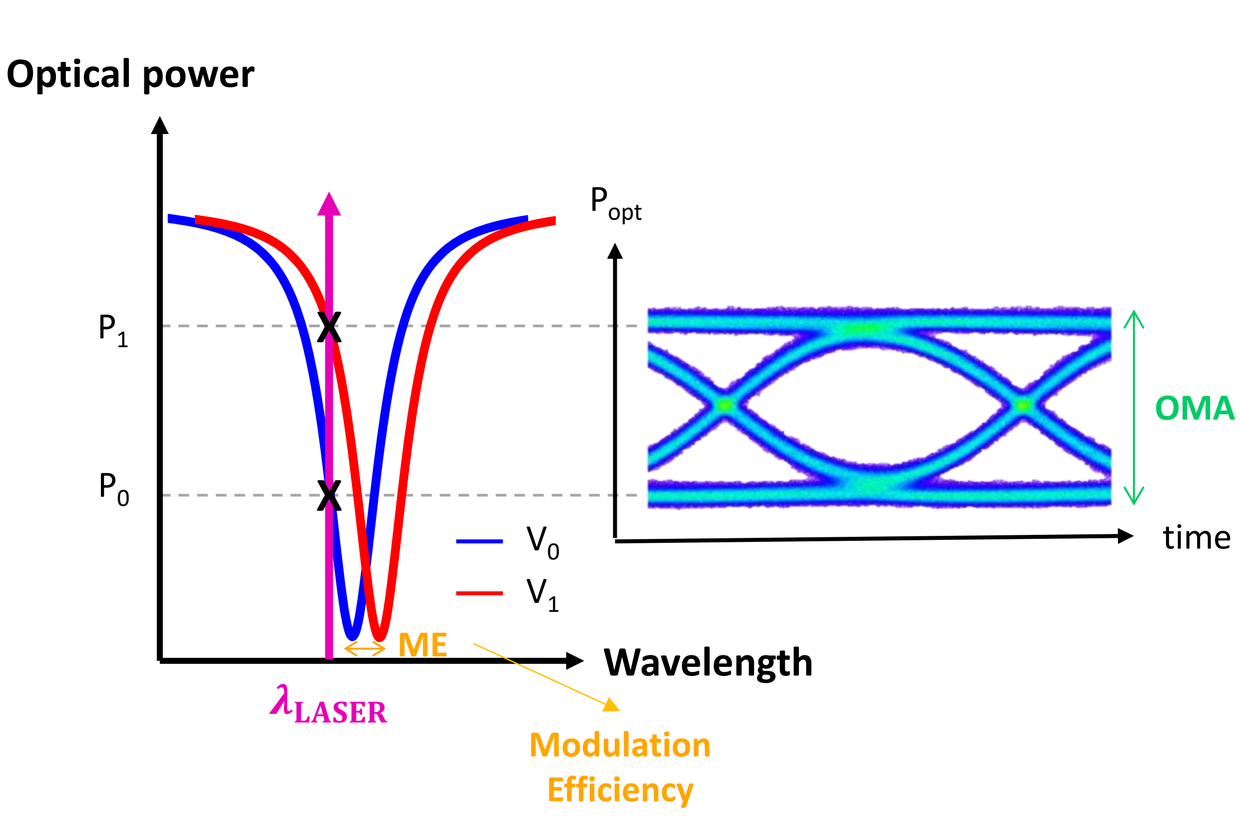

OMA: Optical Modulation Amplitude
ME: Modulation Efficiency

Introduction – Tungsten micro-heaters

- Tungsten µ-heater to shift the resonance wavelength
- **Localized heating**
- Thermo-optic coefficient of silicon stronger than electrical modulation but **slower**

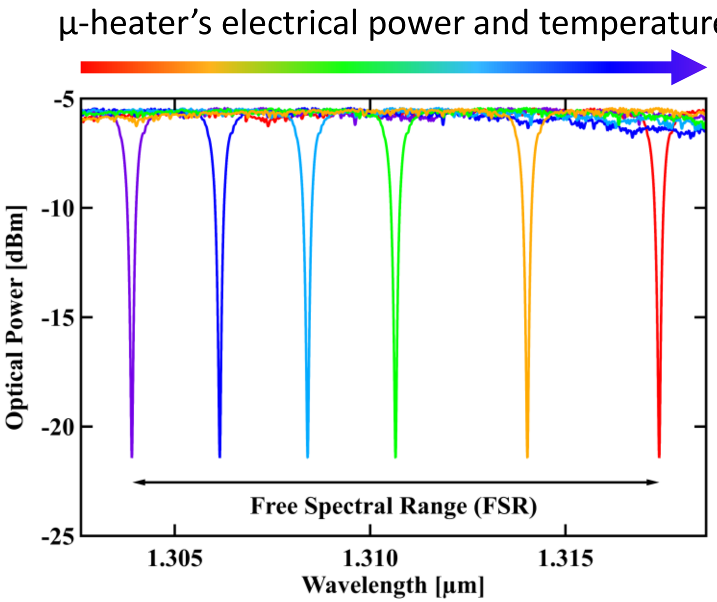

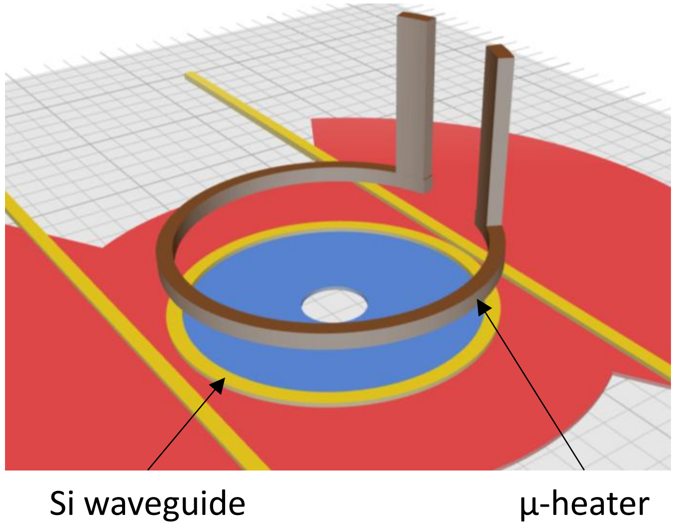

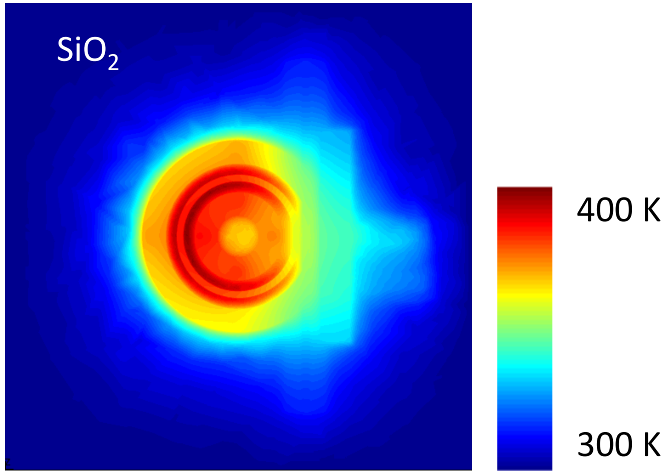

- Thermal shift coefficient of **70 pm/°C** for O-band (1310 nm) and **80 pm/°C** for C-band (1550 nm) ring modulators, significantly larger than the modulation efficiency (~35 pm/V)
- µ-heaters can be used for **localized thermal annealing**

Ring Modulators

X-ray irradiation tests

Total ionizing dose (TID) reached:

$12.3\ MGy\ (SiO_2)$

Irradiation time:

$\sim 9\ days$

Dose rate:

$\sim 55\ kGy/h\ (SiO_2)$

Static Test

- Characterization of ring modulators and photodiodes under ionizing radiation
- **Online acquisition of electrical (I-V) and optical (spectra) device parameters**
- Investigation of temperature effects and thermal annealing post-irradiation

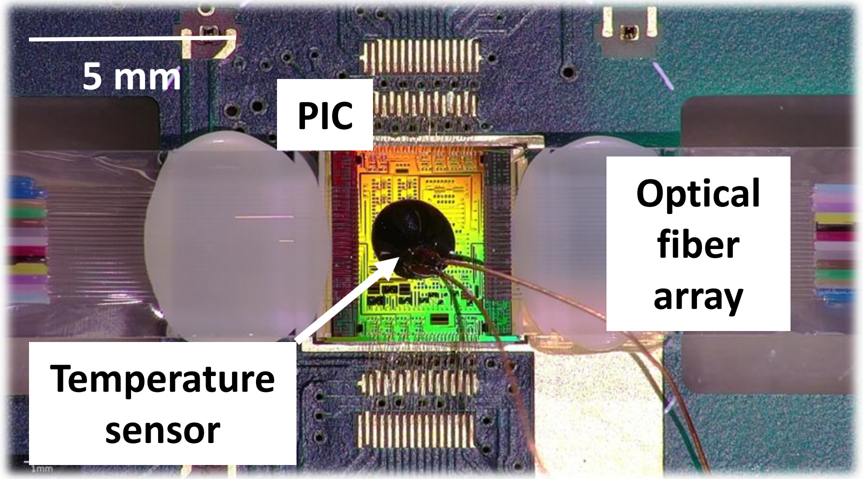

Dynamic Test

- Measurement of **electro-optic (EO) frequency response** of ring modulators under **ionizing radiation**
- Analysis across **different temperatures** and in the **10 MHz - 25 GHz** frequency range
- Investigation of **thermal annealing** during and after irradiation

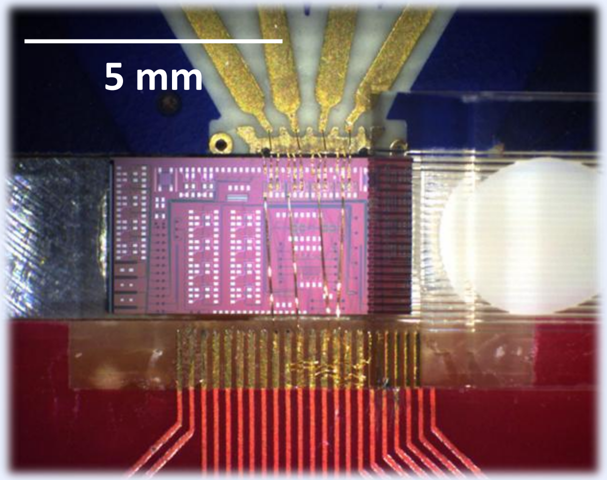

Static X-ray test – Results

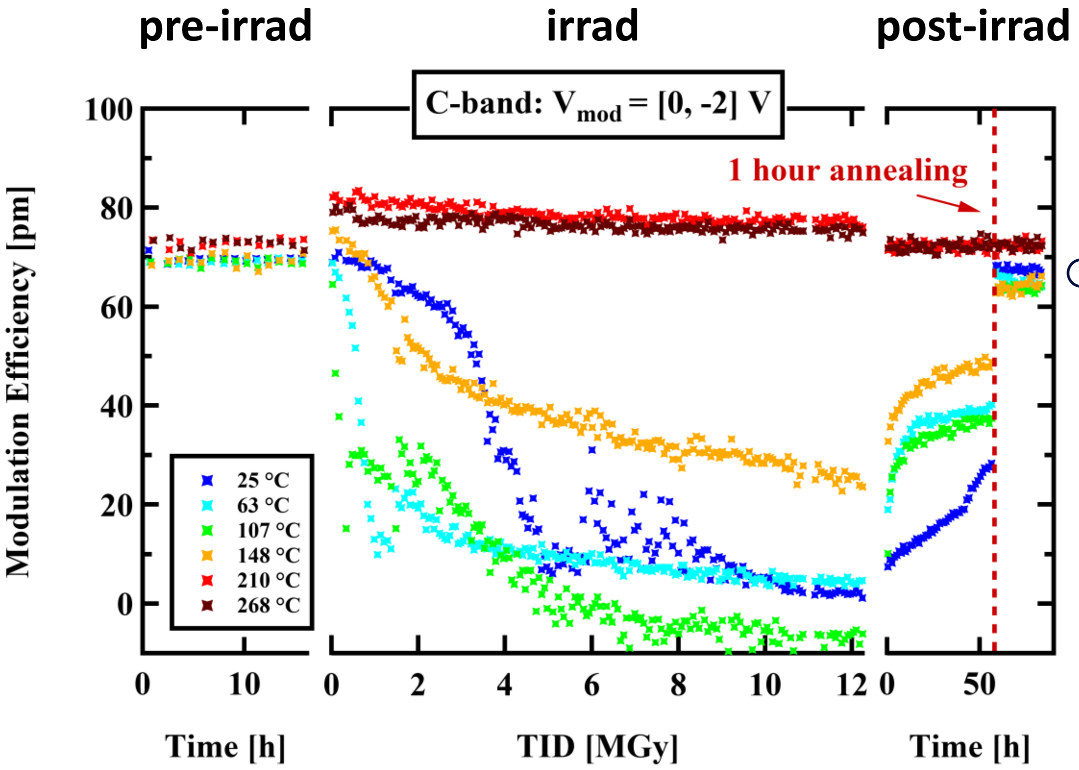

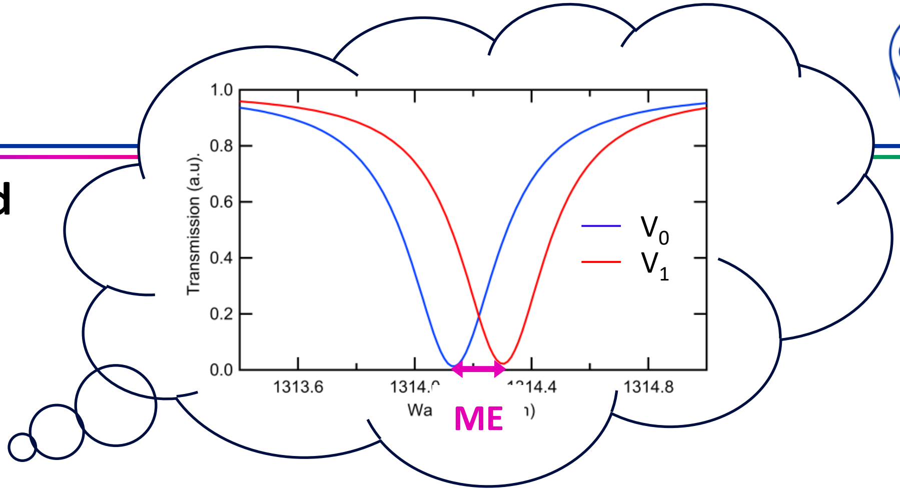

- **Reduction in ME** strongly dependent on temperature
- RMs at **intermediate temperature** range [50°C - 150°C] **degrades faster** than RM at room temperature

✓ One hour annealing at ∼270°C effectively restores ME to pre-irrad values

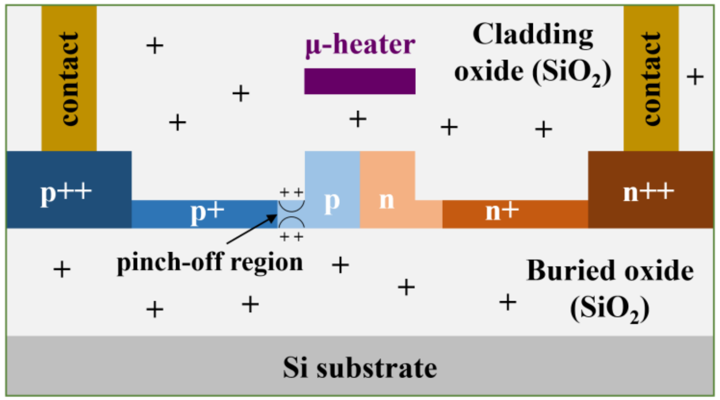

- **Pinch-off of the p-slab caused by positive charge accumulation**
- Increase in the breakdown voltage confirms the pinch-off mechanism

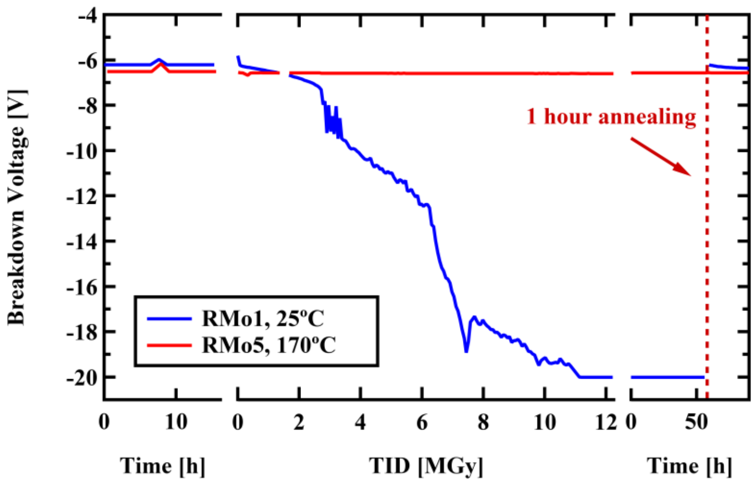

Dynamic X-ray test – EO frequency response (S21)

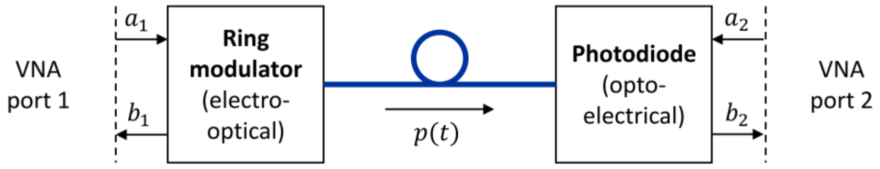

- EO frequency response (S21) measured online using a VNA (Vector Network Analyzer) and a high-speed photodiode

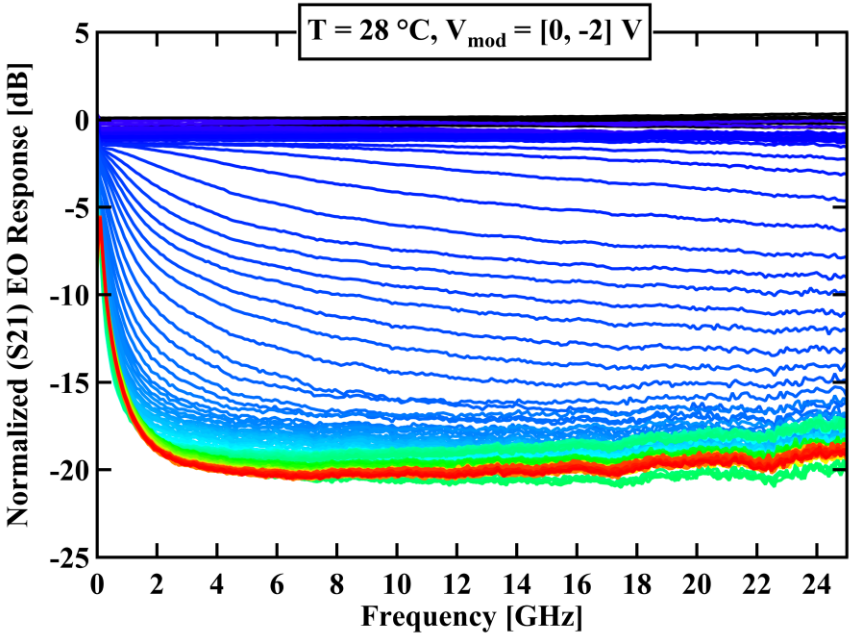

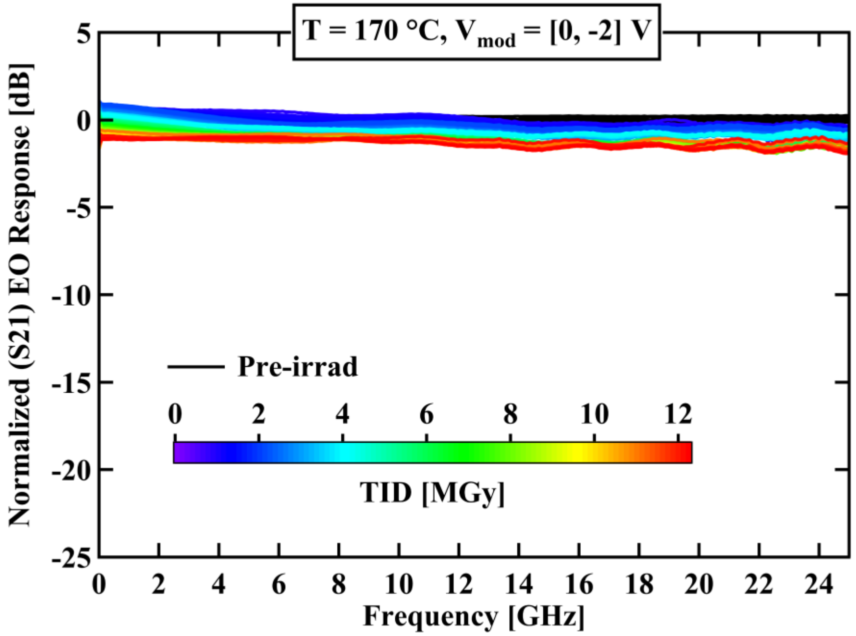

- TID damage is **frequency dependent** and **saturates** around 2 MGy for room temperature device
- RM at **170°C** thanks to the µ-heater **continuously anneal** TID damage

Dynamic X-ray test – S21 at single frequency

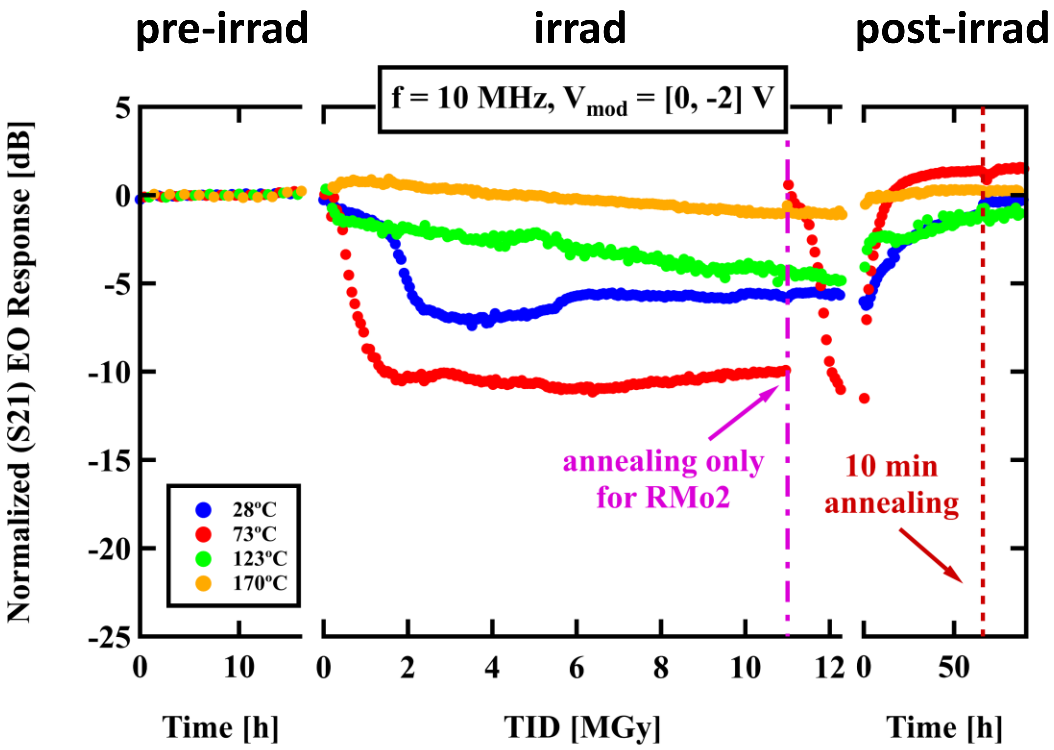

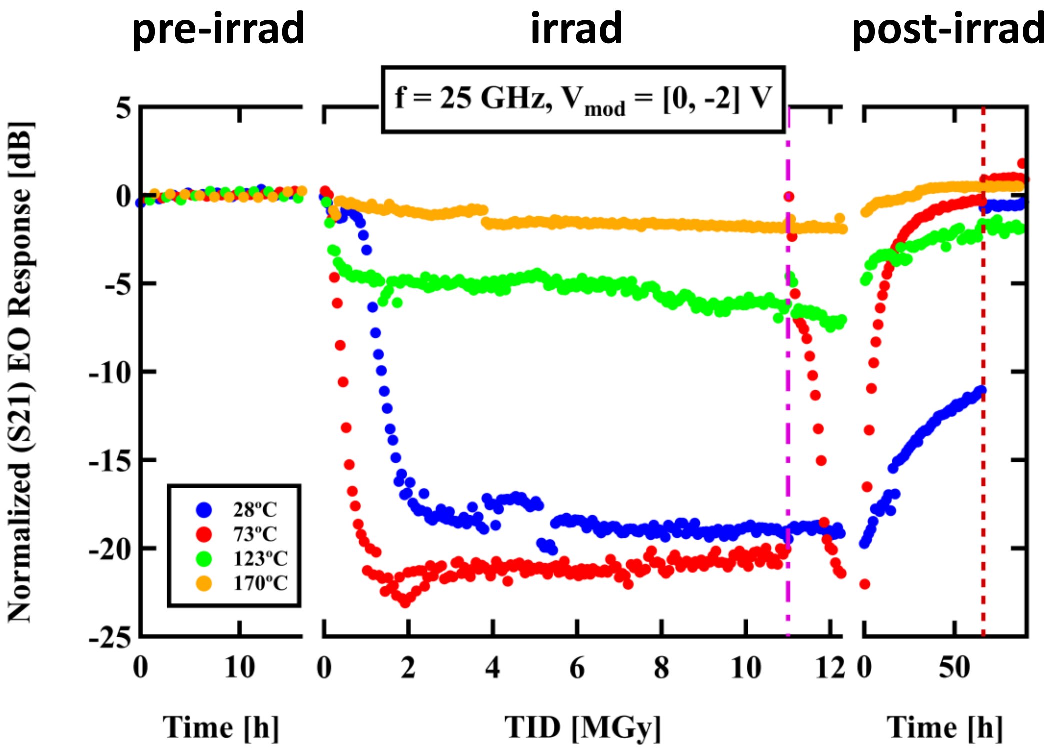

- S21 measurements are consistent with ME results from the static X-ray test:
  - **Faster degradation** observed in the **intermediate temperature** range compared to room temperature device
  - After irradiation, tried **shorter annealing** than in previous test: **10 minutes at 230°C** sufficient to recover the EO frequency response

Dynamic X-ray test – RMo2: annealing during irradiation

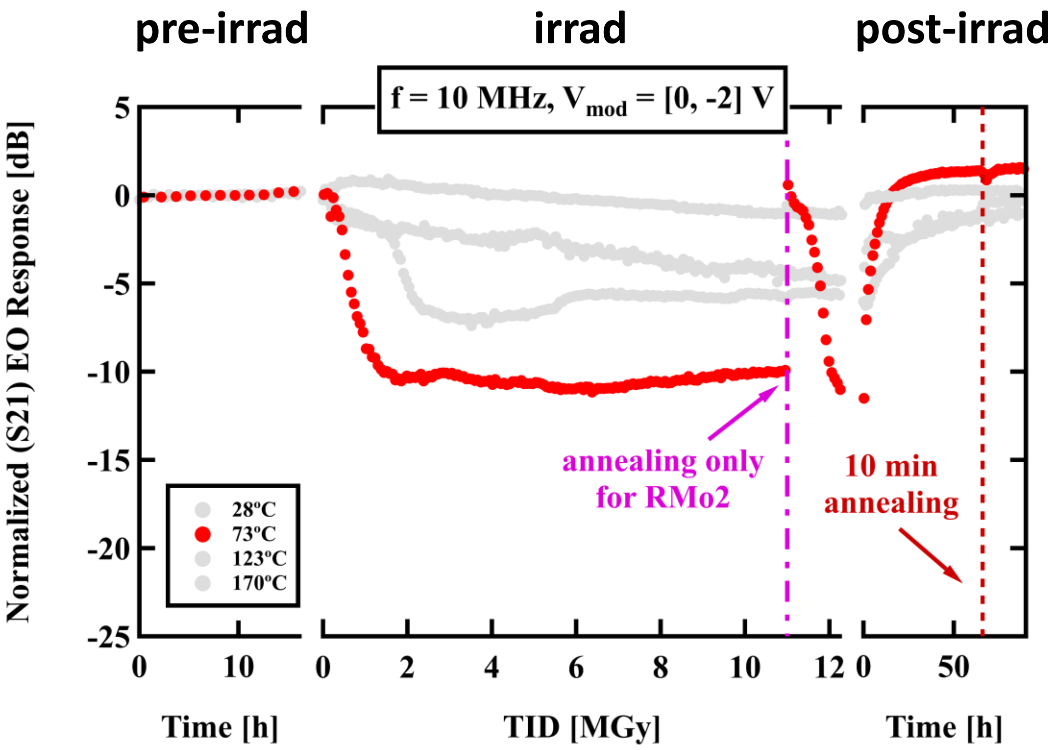

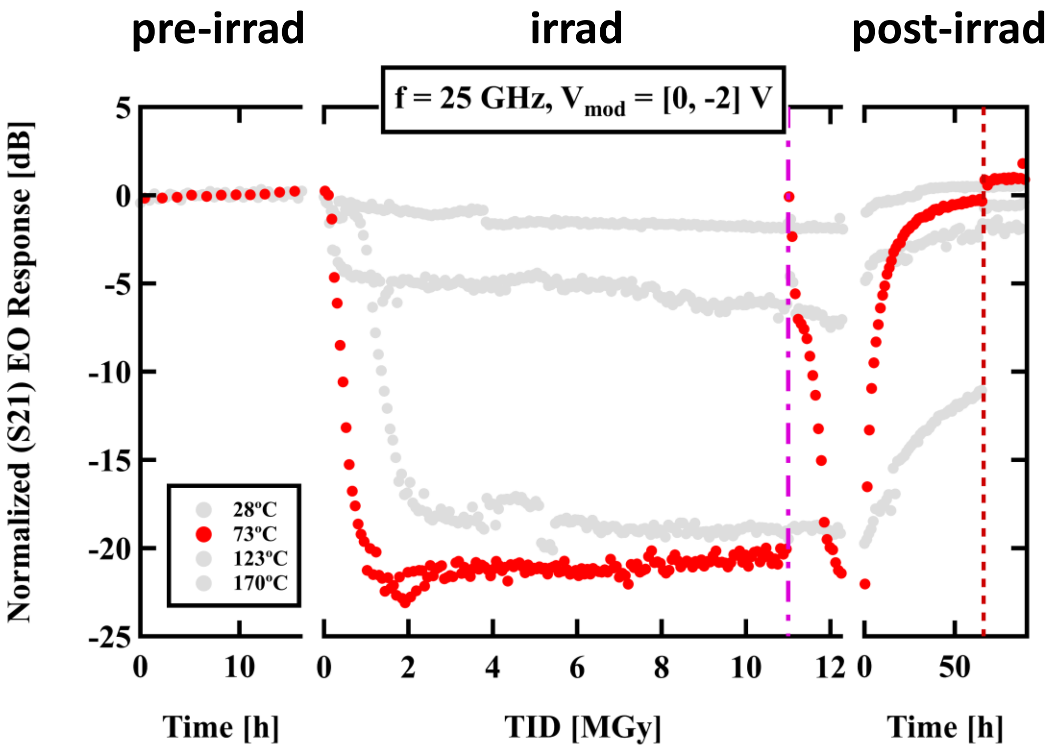

- After reaching the TID target of 10 MGy, a **thermal annealing** step was performed **only** for RMo2 **while keeping irradiating**
- RMo2 (only) kept at **230°C for approximately 30 minutes**, while measurement loop was continuing for other devices
- After the annealing step, **the temperature was lowered back** to 73°C

Dynamic X-ray test – RMo2: annealing during irradiation

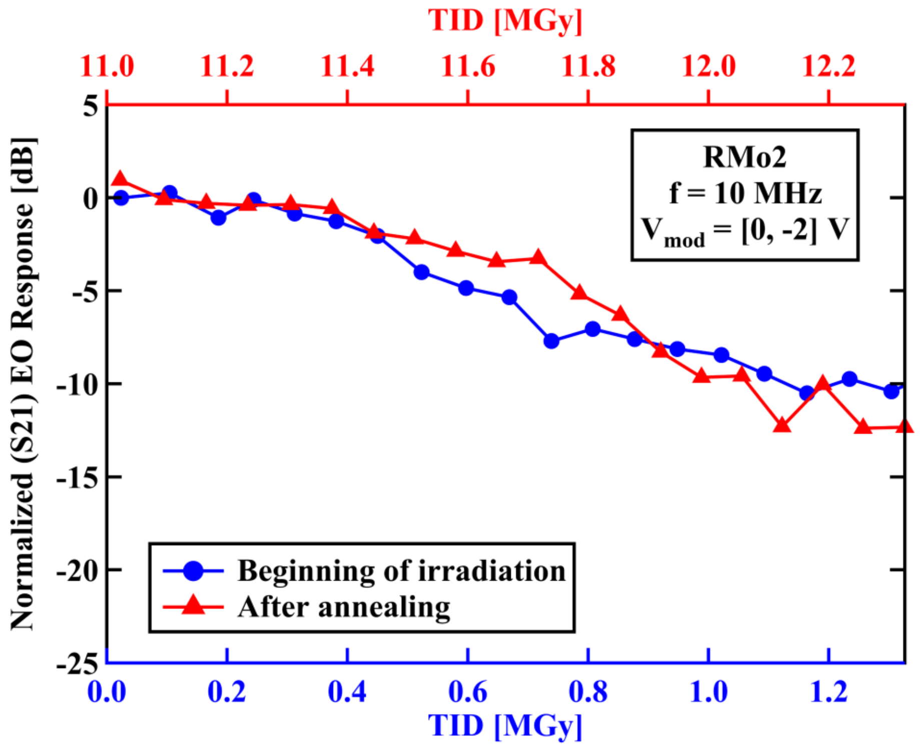

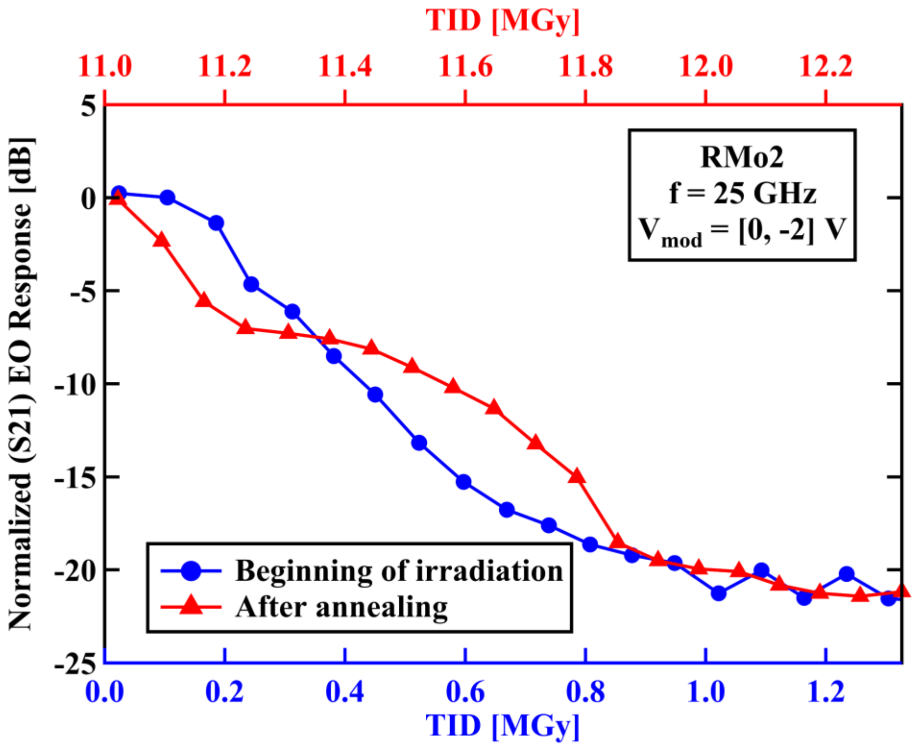

- TID damage resumes following almost the **same degradation trend** as observed at the beginning of the irradiation

✓ After localized thermal annealing, **radiation damage does not accumulate** with previous one

Dynamic X-ray test – Eye diagrams

- Eye diagrams at 25 Gbps were acquired from the irradiated sample and compared with those from non-irradiated devices

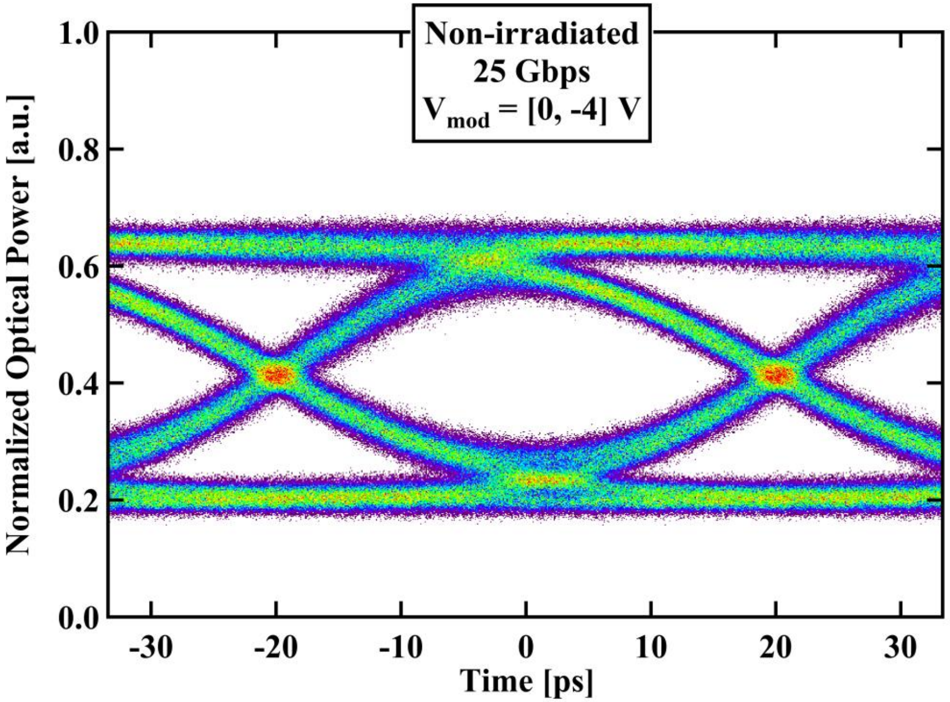

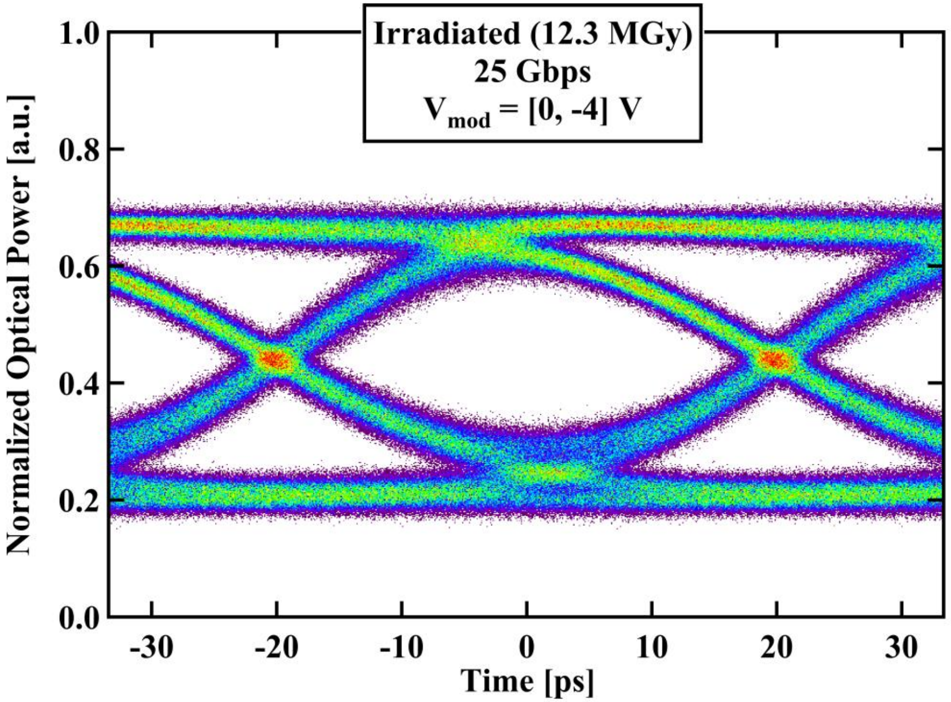

✓ **No evidence of degradation** after thermal annealing

✓ Eye diagram parameters do not show differences compared to non-irradiated ring modulators

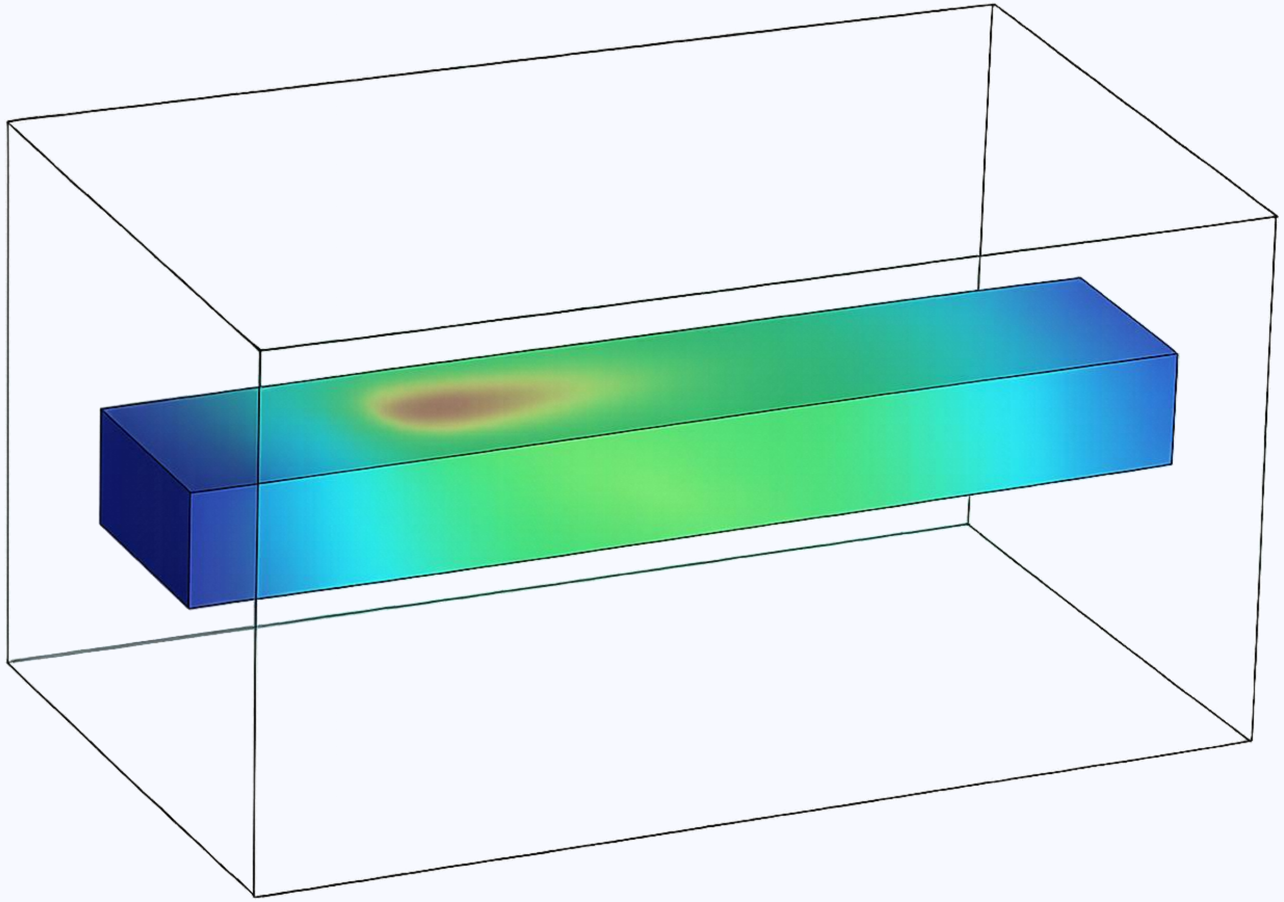

Waveguides

Irradiation campaigns and TCAD simulations

Neutron test – Setup

- Evaluation of **radiation-induced attenuation (RIA) in SiPh waveguides**
- Measurements of different waveguide types in the two optical bands (O-band at 1310 nm and C-band at 1550 nm)

Neutron fluence reached:

$7 \times 10^{15}\ n/cm^2$

Peak beam neutron energy:

$23\ MeV$

Irradiation time:

$\sim 34\ hours$

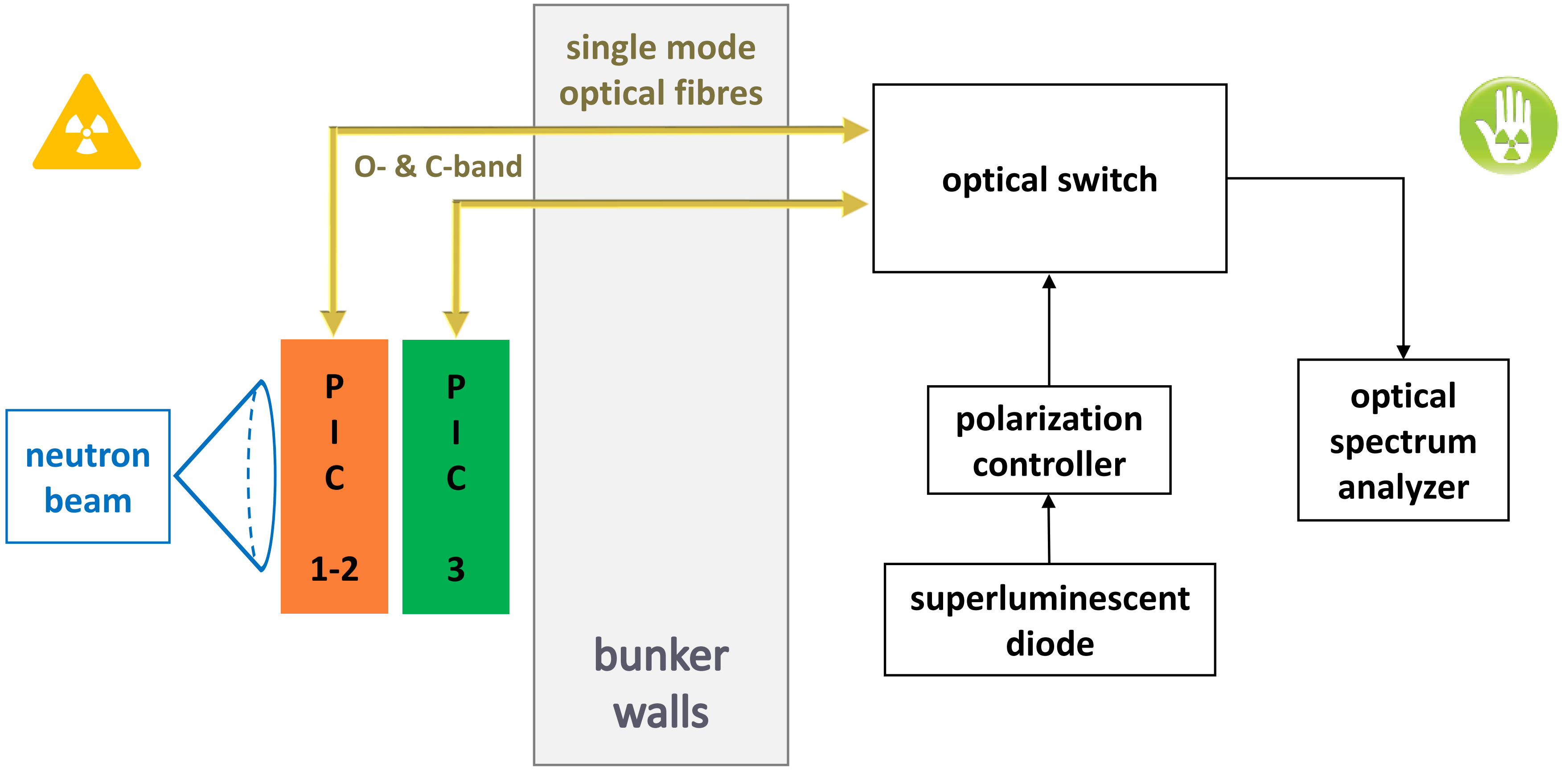

Neutron test – Optical transmission spectra measurements

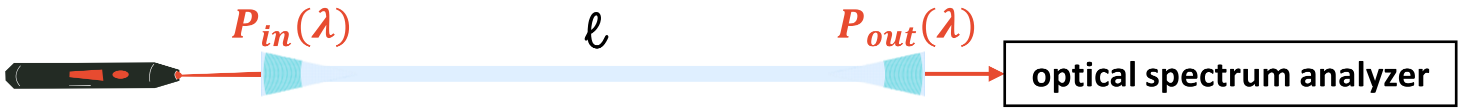

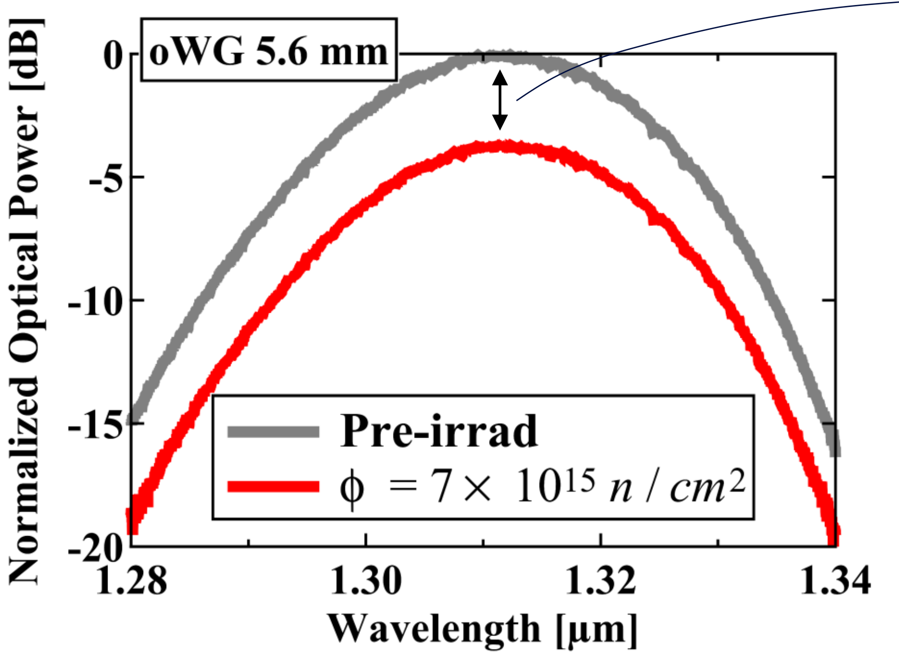

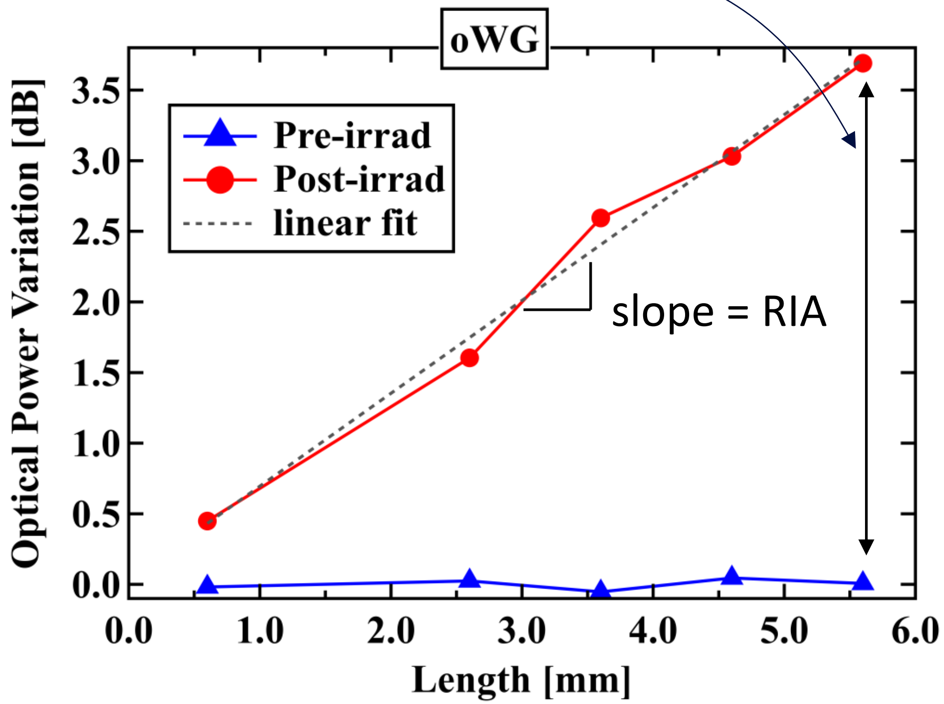

- Linear fit for the calculation of the RIA ('cut-back' method)
- The **variation of the slope** gives the **RIA**
- The variation of the y-intercept gives the variation in the grating coupler response (if any)

Neutron test – RIA in waveguides

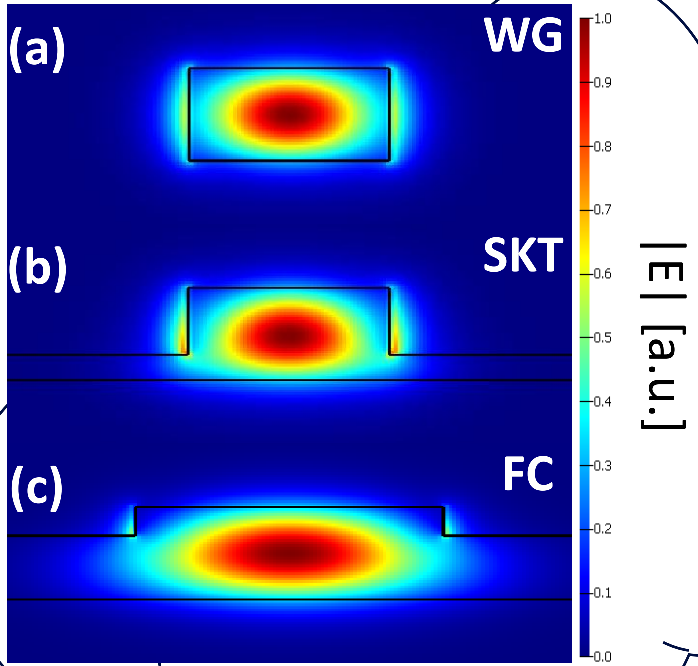

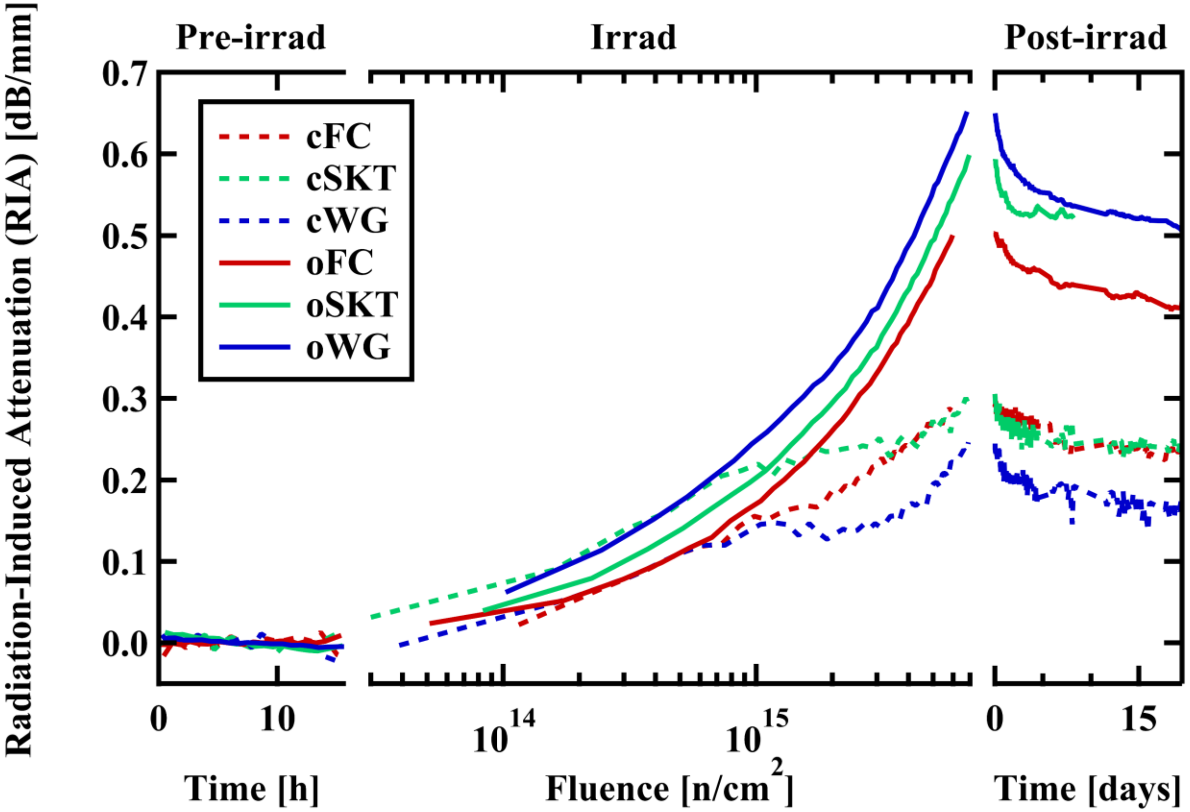

- Waveguides in O-band show a higher RIA than their counterpart in the C-band
- Attention must be taken when designing a PIC

Neutron test – Explaining the results

- **Displacement damage (DD)**

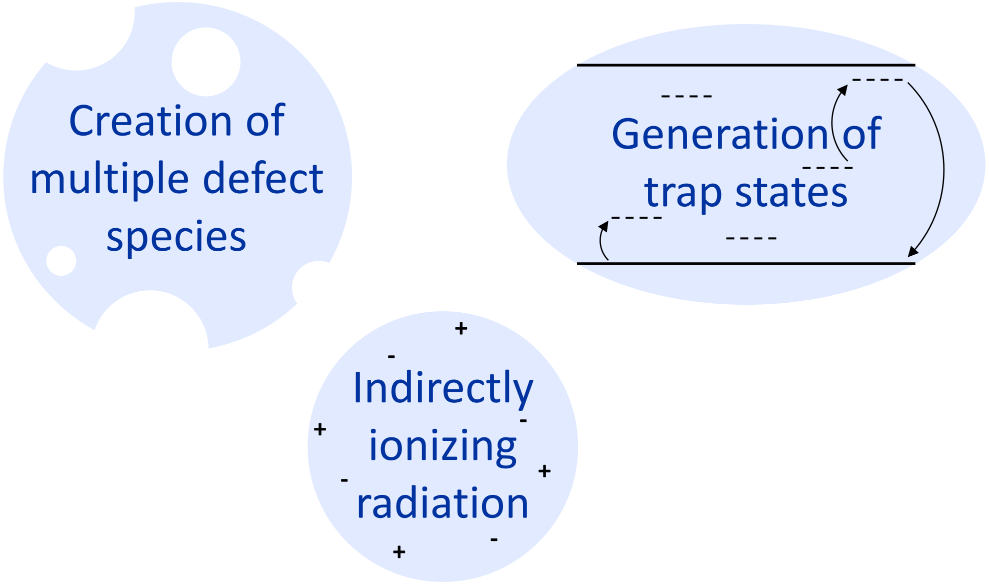

- Both studies show a larger increase in the absorption coefficient at 1310 nm compared to 1550 nm

$$E\big|_{eV} = \frac{1.24}{\lambda|_{\mu m}}$$

- Defected-induced energy states reduce the optical absorption length

C. Scharf, F. Feindt, and R. Klanner, “Influence of radiation damage on the absorption of near-infrared light in silicon,” *Nuclear Instruments and Methods in Physics Research Section A: Accelerators, Spectrometers, Detectors and Associated Equipment*, vol. 968, p. 163955, 2020. [Online]. Available: https://www.sciencedirect.com/science/article/pii/S0168900220304277

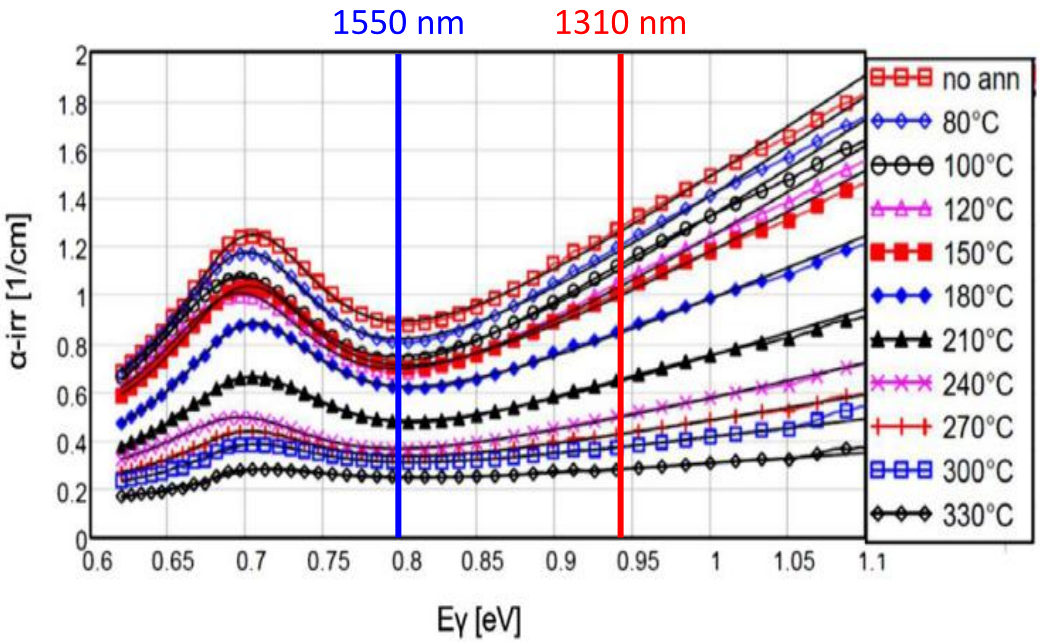

E. Fretwurst, R. Klanner, J. Schwandt, and A. Vauth, “Study of the v20 state in neutron-irradiated silicon using photon-absorption measurements,” *Nuclear Instruments and Methods in Physics Research Section A: Accelerators, Spectrometers, Detectors and Associated Equipment*, vol. 1053, p. 168353, 2023. [Online]. Available: https://www.sciencedirect.com/science/article/pii/S0168900223003431

X-ray test – RIA in waveguides

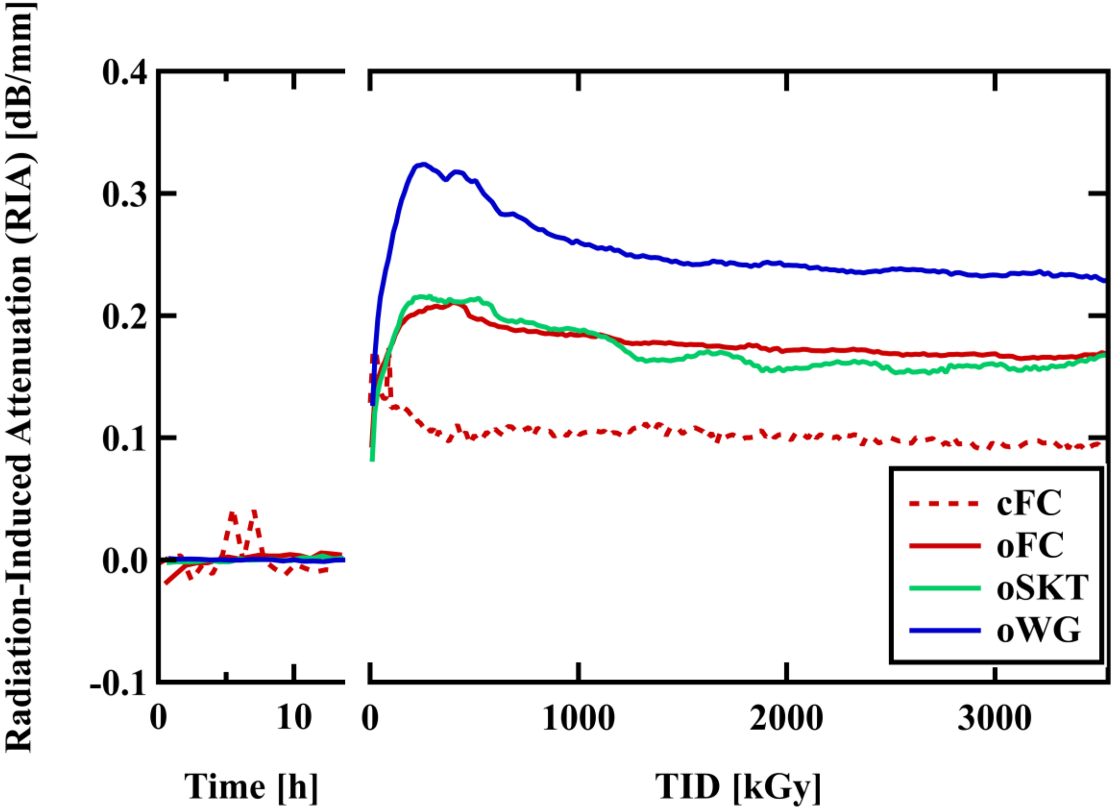

- Same setup as for the neutron test
- X-ray test to **decouple the RIA from non-ionizing and ionizing radiation**
- **RIA saturates**, confirming our previous measurements and some results found in literature

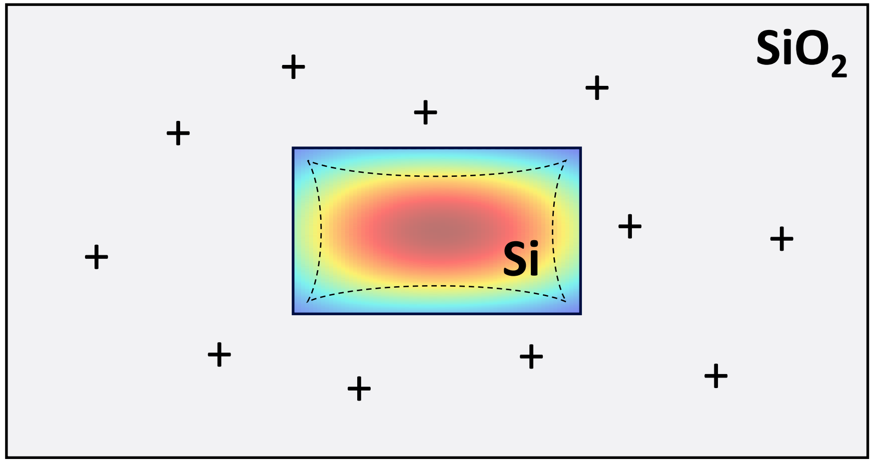

- Hypothesis: the accumulation of positive charges in the SiO_2 and at the Si/SiO_2 interface pushes free carriers in the waveguide (slightly p-doped) toward the center, increasing their **overlap with the optical mode** and enhancing absorption due to free-carrier absorption

Many thanks to Carlos Solans Sanchez and the ATLAS Tracking Detectors (EP-ATL-TRK) group for providing access to their X-ray facility, and to Kourosh Sarbandi for assistance with the dosimetry!

Heavy ion test – Setup

- Evaluation of **optical single-event transients (OSETs)** in SiPh waveguides
- **First heavy-ion test for OSETs** (no tests for OSETs have been reported in the literature)

Max. LET available from the ion cocktail:

$61.3\ MeV \cdot cm^2/mg$

Ion flux:

$15000\ ions/s \cdot cm^2$

Angles of incidence:

$0° - 45° - 75°$

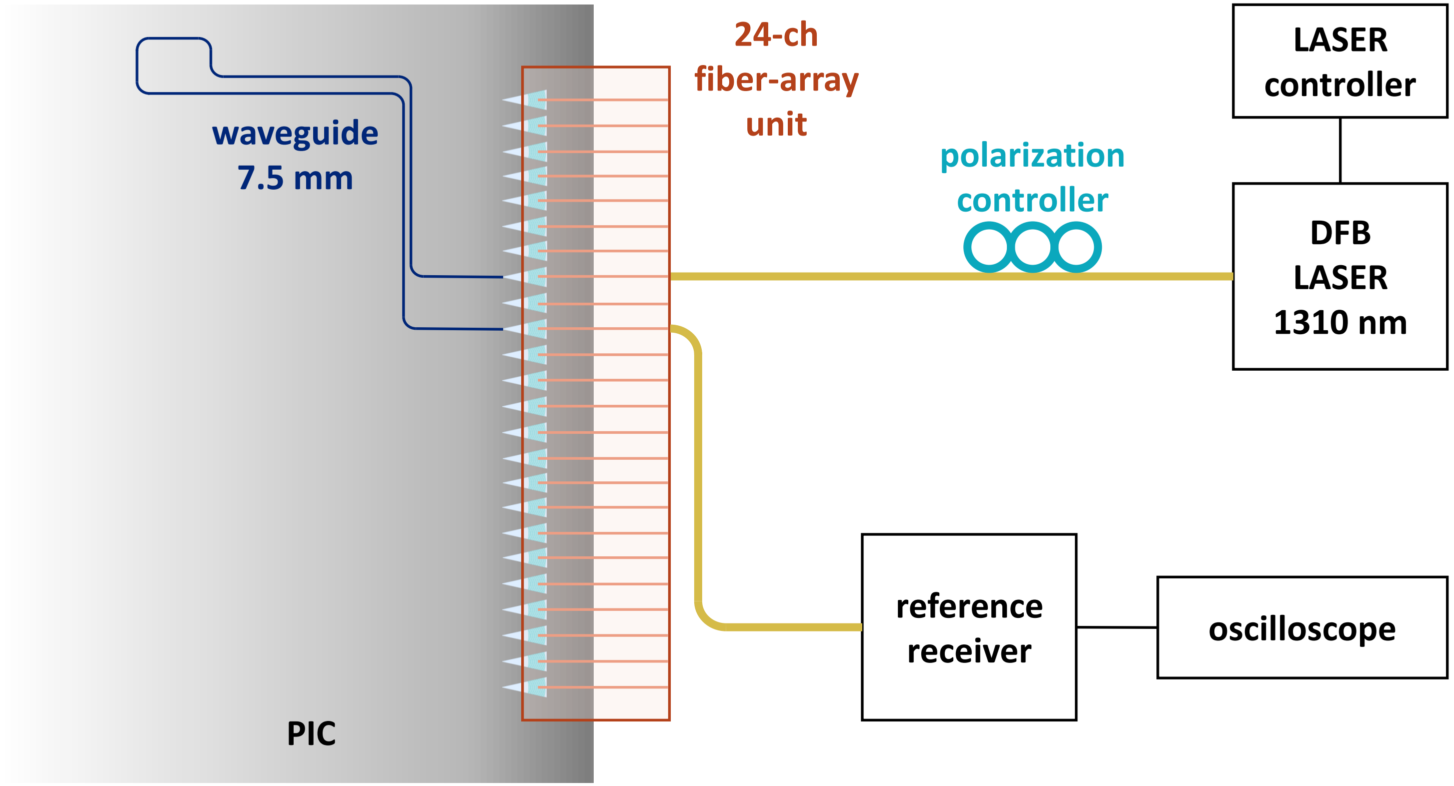

This activity has received funding from the European Union's 2020 research and innovation programme under grant agreement No 101008126, corresponding to the ***RADNEXT*** *project.*

Heavy ion test – What is an OSET?

OSET: single-event transient in the optical domain

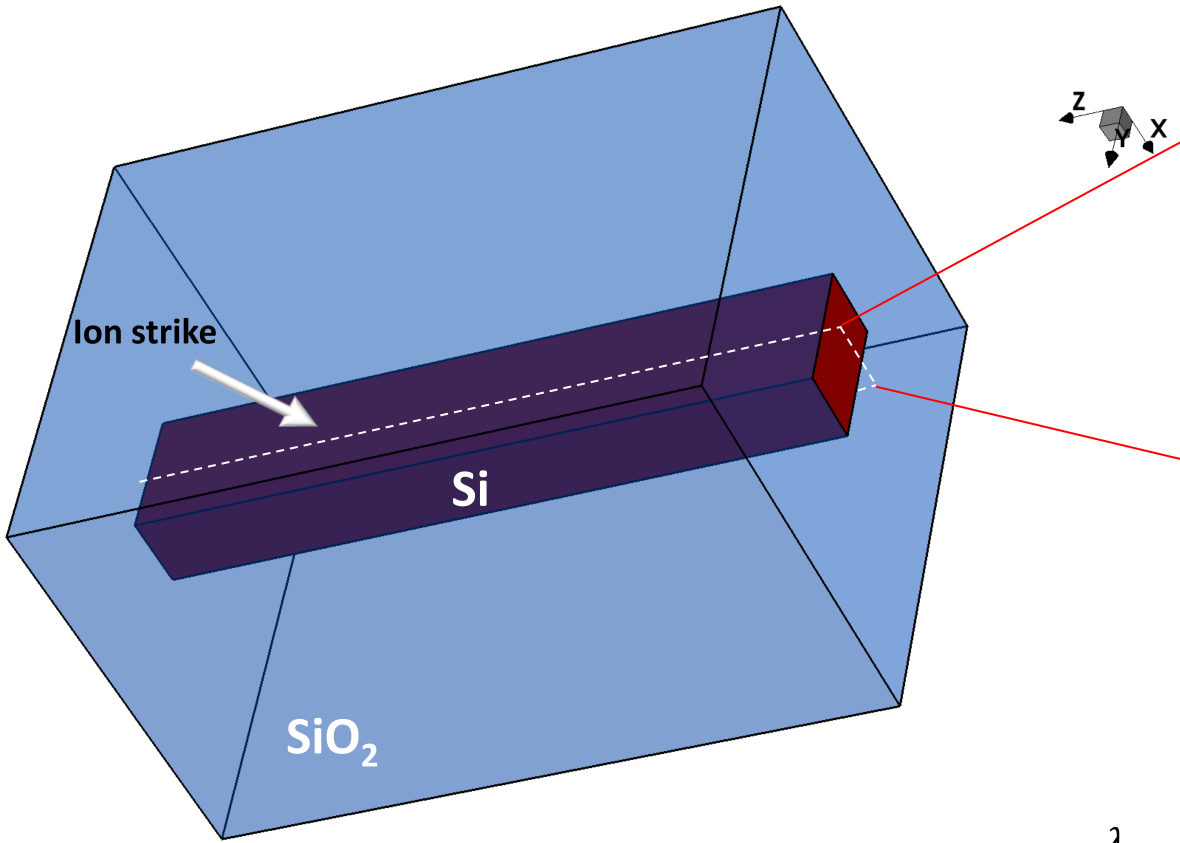

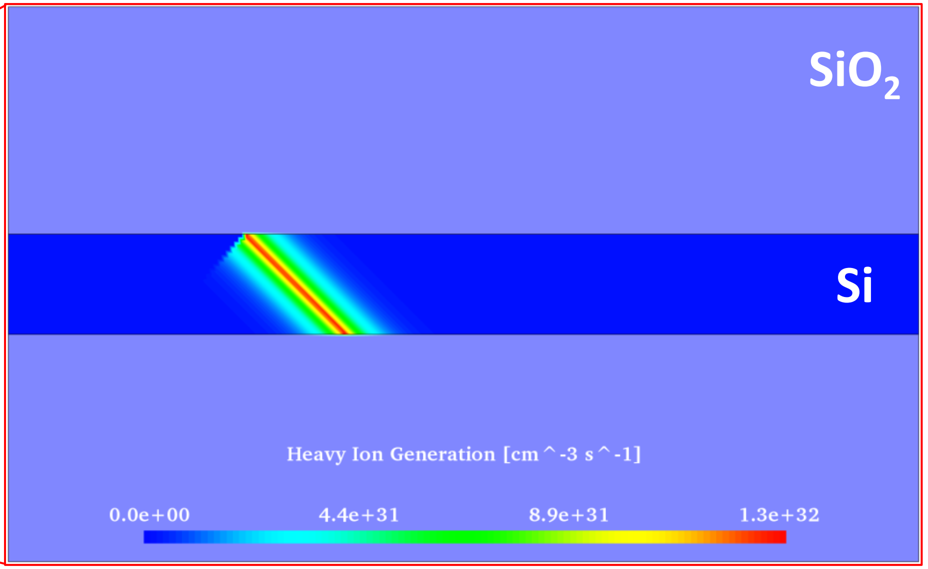

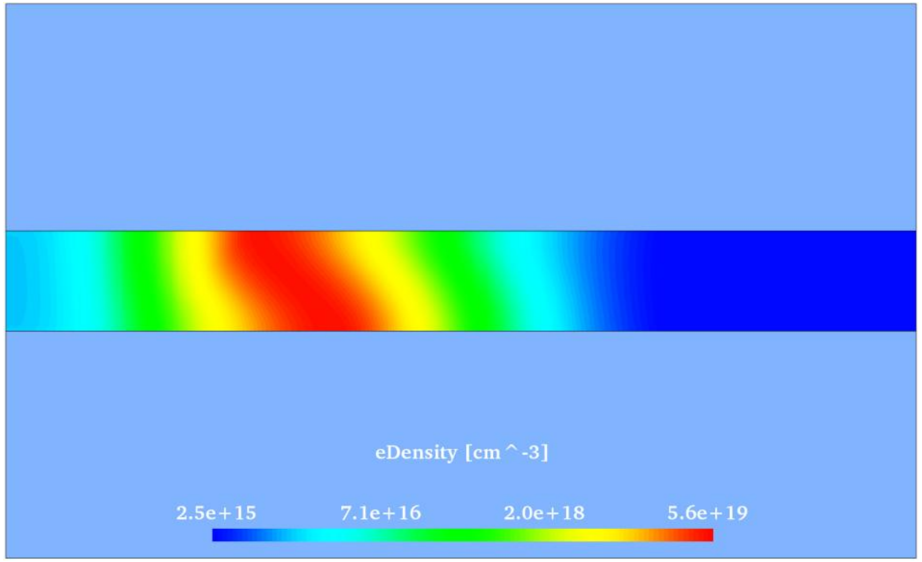

$$n(\lambda, N_e, N_h) = n_0(\lambda) + \Delta n_{fc}(N_e, N_h) - i\frac{\lambda}{4\pi}\Delta\alpha_{fc}(N_e, N_h)$$

$$absorption\ (\Delta\alpha) \propto (\Delta N_{\text{electrons}} + \Delta N_{\text{holes}})$$

Heavy ion test – What is an OSET?

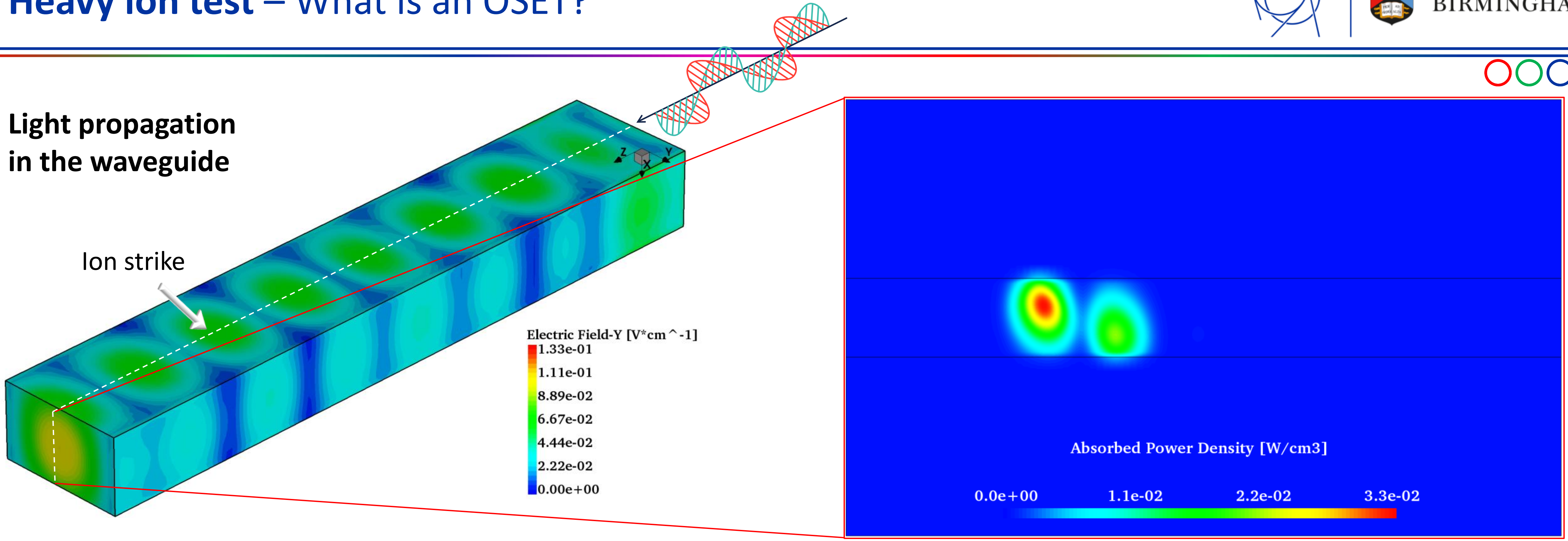

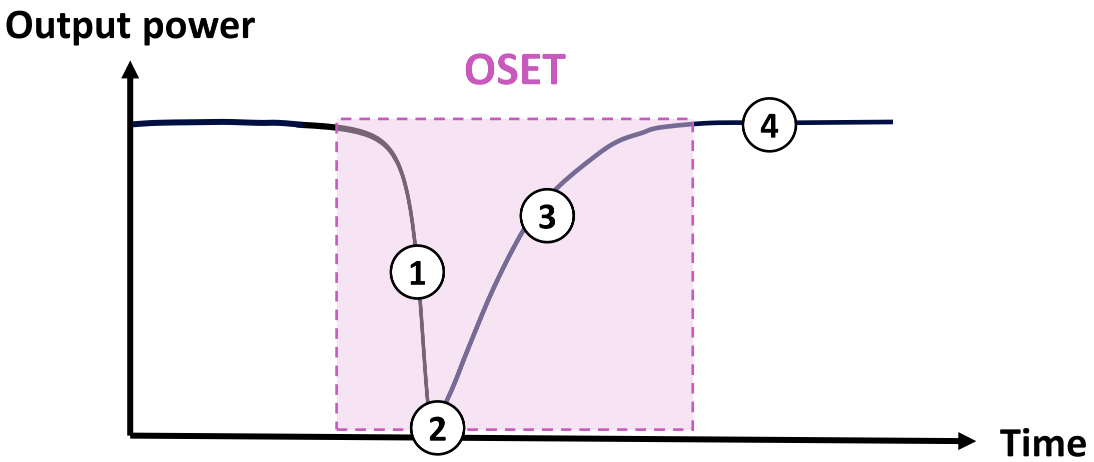

1. Initial carrier generation from ion strike [100 ps to 1 ns]
2. Peak of carrier generation and optical attenuation
3. Recombination mechanisms [tens of ns]
4. Complete recovery from the transient event [after ~100 ns]

(unit interval for a bit at 25 Gbps is 40 ps)

Heavy ion test – Measurements

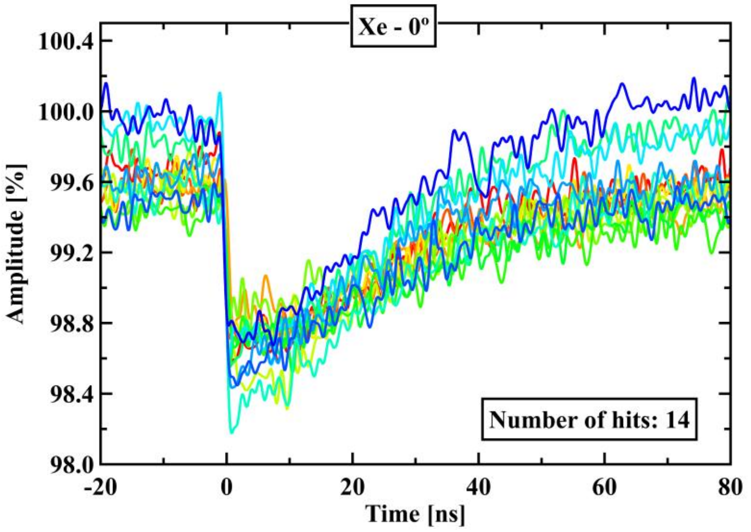

- For perpendicular strike, OSETs were observed only for the heaviest ion ($^{124}Xe^{35+}$, LET of 61.3 MeV·cm^2/mg)
- The ratio was approximately of 1 hits/min, with maximum amplitude of transient of ~1.5 %
- **Maximum transient amplitude of ~4 %** with highest LET and angle of incidence of 75°
- Two-peaks distribution of the transient amplitude because of the L-shaped waveguide

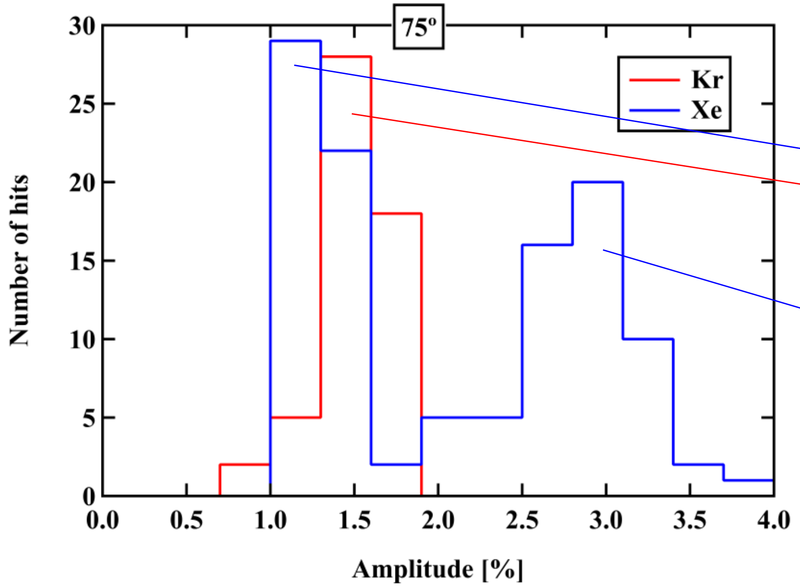

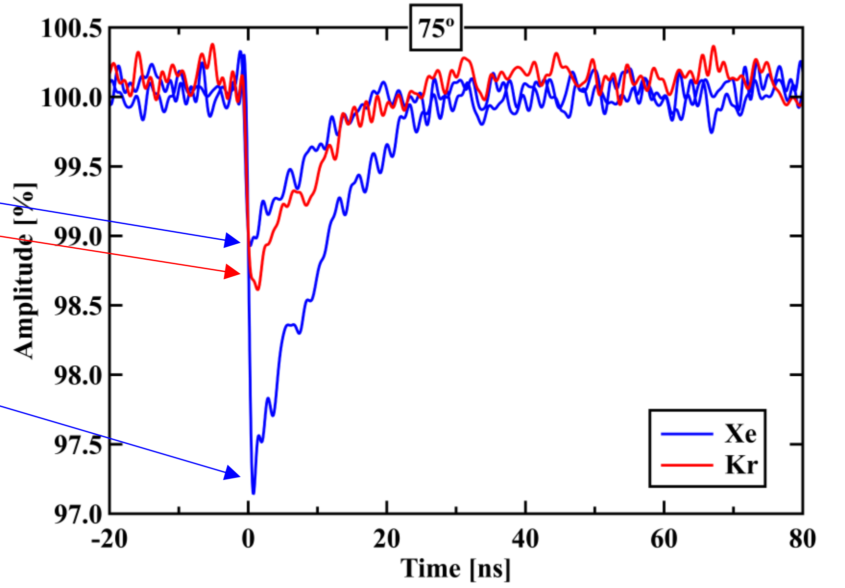

Heavy ion test – TCAD simulations

- Sentaurus TCAD is a powerful tool to combine:
  - **Electrical simulations** → carrier generation, diffusion and recombination from the heavy ion strike (**variation in the complex refractive index** due to the different number of carriers)
  - **Electromagnetic simulations** → finite-difference time-domain (**FDTD**) solver to compute the electromagnetic field propagation

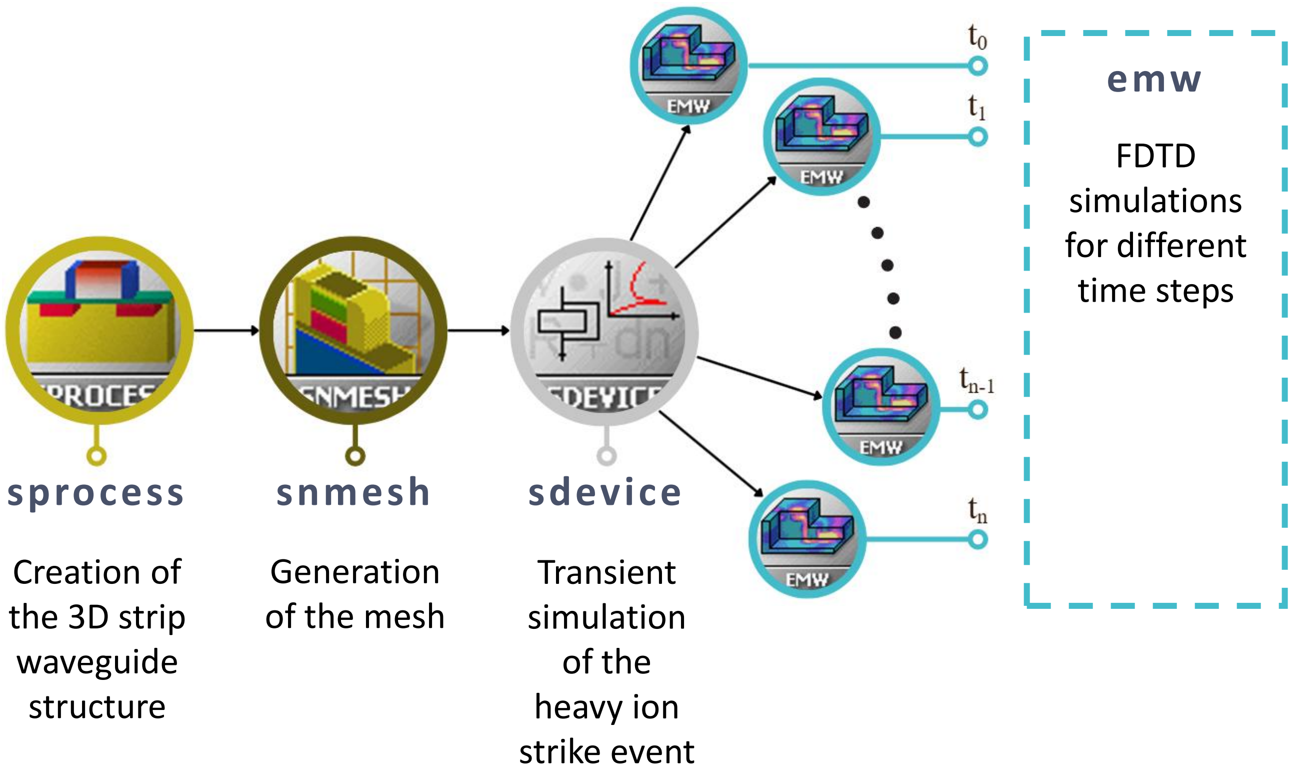

Heavy ion test – TCAD simulations

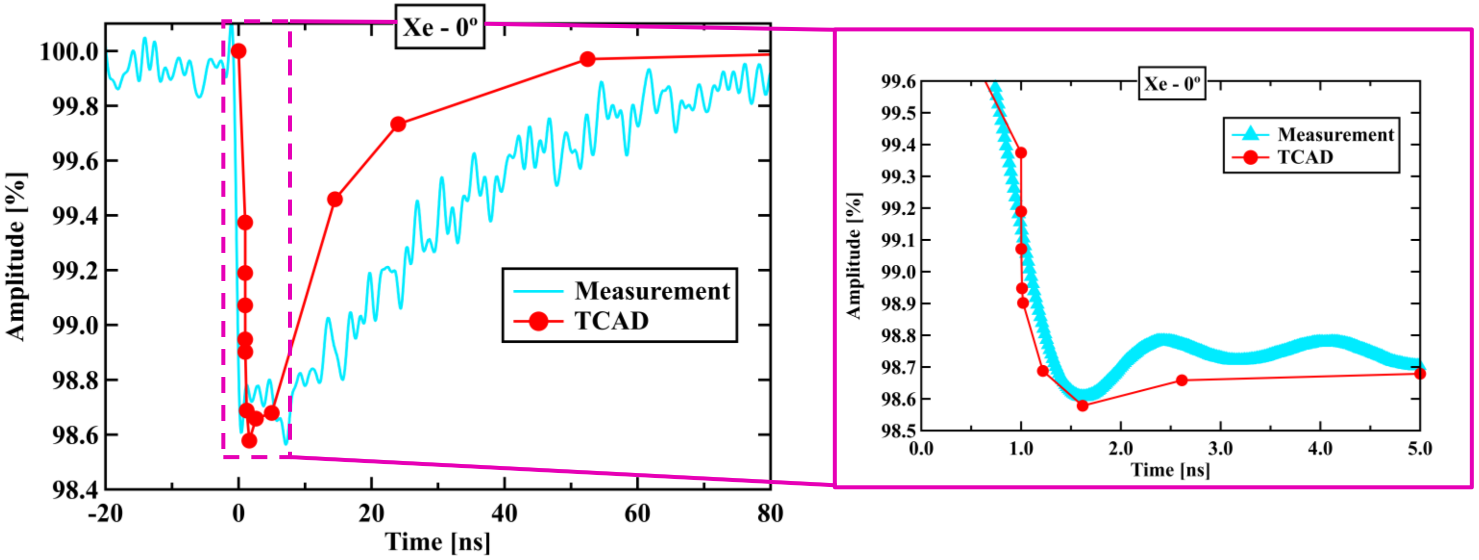

- Starting from the LET of 61.3 MeV·cm^2/mg we can set a defined number of electron-hole pairs generated per volume within the TCAD simulation (details of the calculations in the backup)
- **Amplitude of the transient matches well the measurements**
- Good match also for the left-hand side of the transient (initial charge generation)

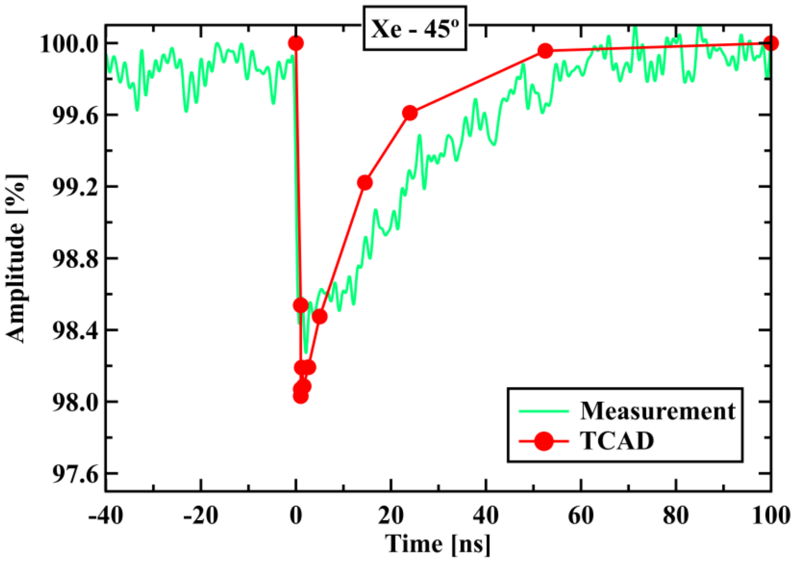

- The transient amplitude shows a **good matching also when the angle of incidence is changed**
- **Overestimation of the recombination time constant** (for now used the pre-defined TCAD values, trying with different recombination parameters)

Heavy ion test – Surface recombination

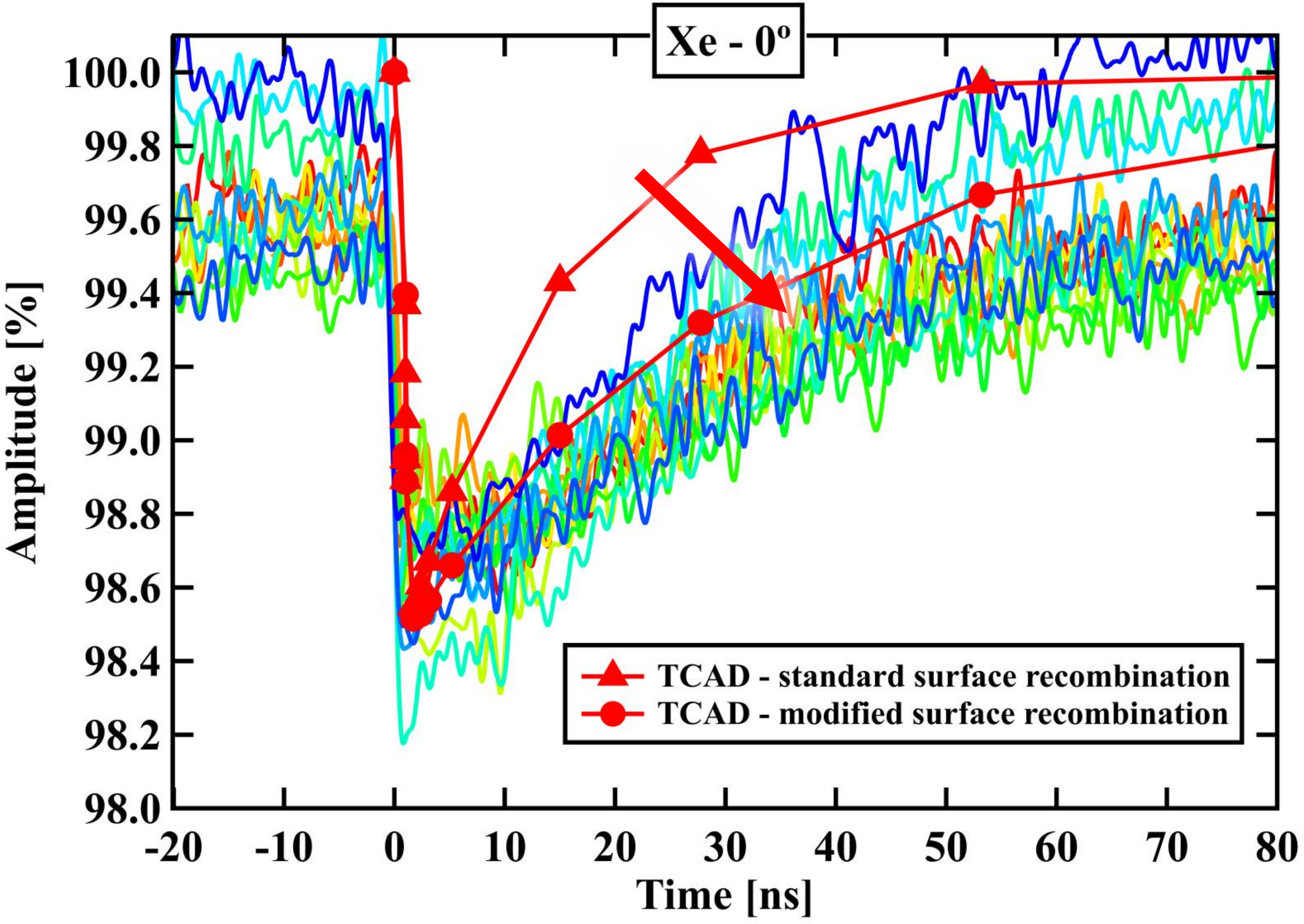

$$s = s_0\left[1 + s_{\mathrm{ref}}\left(\frac{N_{\mathrm{i}}}{N_{\mathrm{ref}}}\right)^{\gamma}\right]$$

- By reducing the surface recombination velocity from the default value, we match not only the amplitude of the OSET but also the typical recovery time

Conclusions…

- **Dynamic X-ray irradiation test** on SiPh **ring modulators** have demonstrated the susceptibility of the electro-optic frequency response to TID damage (pinch-off mechanism of the silicon slab).

- **Localized thermal annealing** using the built-in micro-heaters **restores completely the performance**. No sign of degradation in the eye diagrams after thermal annealing.

- **Neutron** and **X-ray irradiation tests** on SiPh **waveguides** highlighted evidence of **radiation-induced attenuation** that must considered for future PIC designs.

- **Heavy ion** testing demonstrated **non-significant influence of OSETs** in the SiPh waveguides transmission. Transient amplitude with LET up to 61.3 MeV·cm^2/mg and angle of incidence of 75° remained **below 4 %**.

- **TCAD simulations of OSETs events** show a good agreement with the measured transient, both in amplitude and recombination time.

…and future work

- Write the thesis 🫠

daniele.alfiero@cern.ch

Thank you for your attention!

Backup

Optical datalinks in High-Energy Physics

- Optical data link are vital parts of modern High Energy Physics (HEP) experiments
  - CERN experiments exploit tens of thousands of custom optical datalinks
- All these links utilize conventional discrete components
  - Directly modulated lasers and normal-incidence p-i-n photodiodes
  - Mature technologies and thoroughly studied characteristics under irradiation
- We are reaching the limits what can be done with conventional links: few × 10^{15} n/cm^2
- The placement already restricted by radiation levels during the experiment lifetime

The final runs of High-Luminosity LHC and future accelerators require even higher levels of radiation tolerance

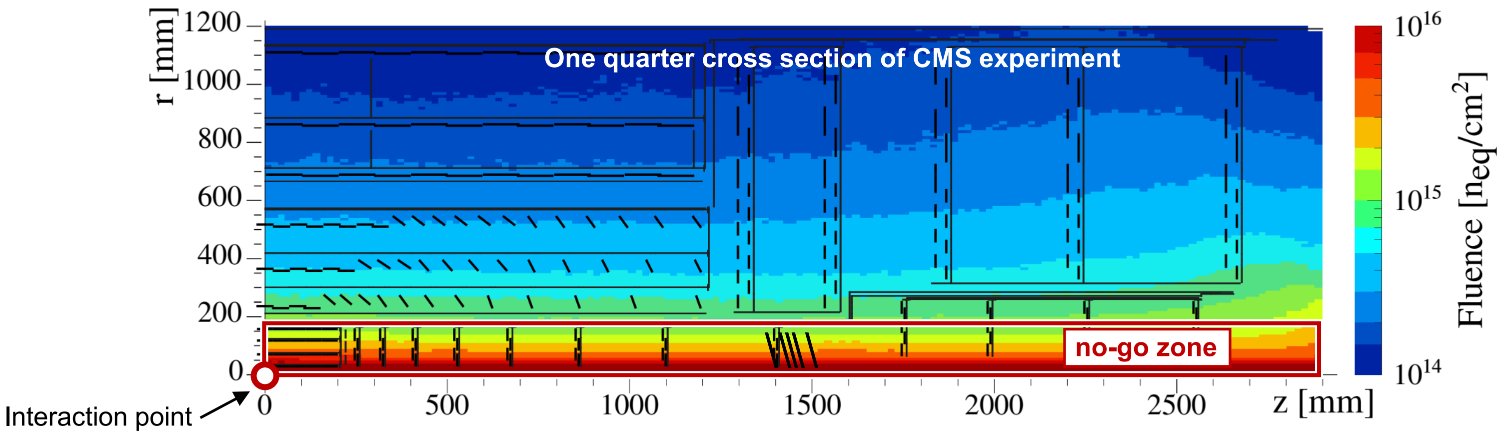

Integrated particle fluence in 1 MeV neutron equivalent per cm^2, for the CMS Phase-2 tracker.
[The Phase-2 Upgrade of the CMS Tracker]

Introduction – Ring Modulators

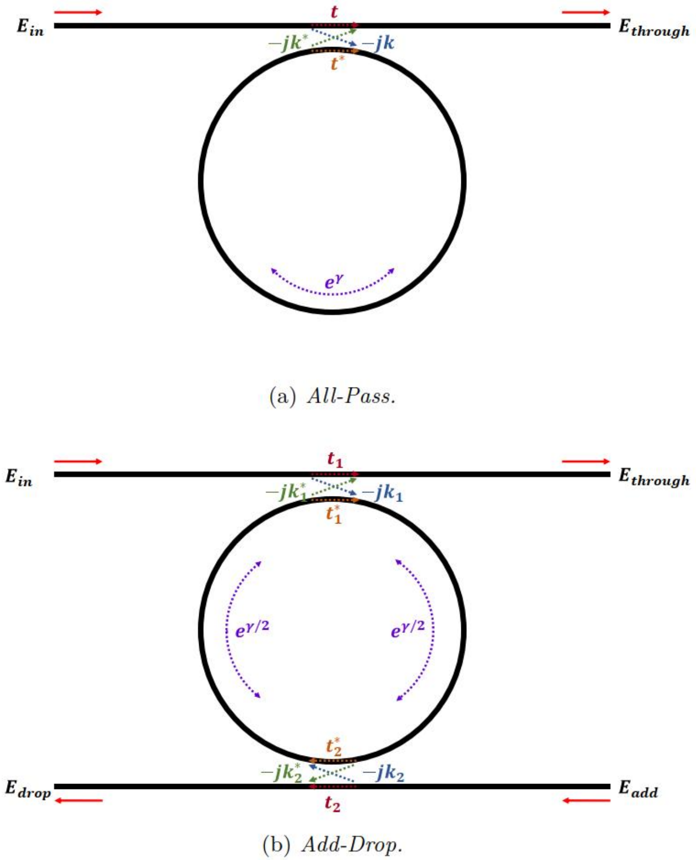

Figure 1.5: (a) All-pass and (b) add-drop configurations of the ring resonator, with the coefficients for the evanescent and transmitted electromagnetic fields.

$$\Delta n = \Delta n_e + \Delta n_h = -\left[8.8 \cdot 10^{-22} \Delta N_e + 8.5 \cdot 10^{-18} (\Delta N_h)^{0.8}\right],$$

$$\Delta \alpha = \Delta \alpha_e + \Delta \alpha_h = 8.5 \cdot 10^{-18} \Delta N_e + 6.0 \cdot 10^{-18} \Delta N_h,$$

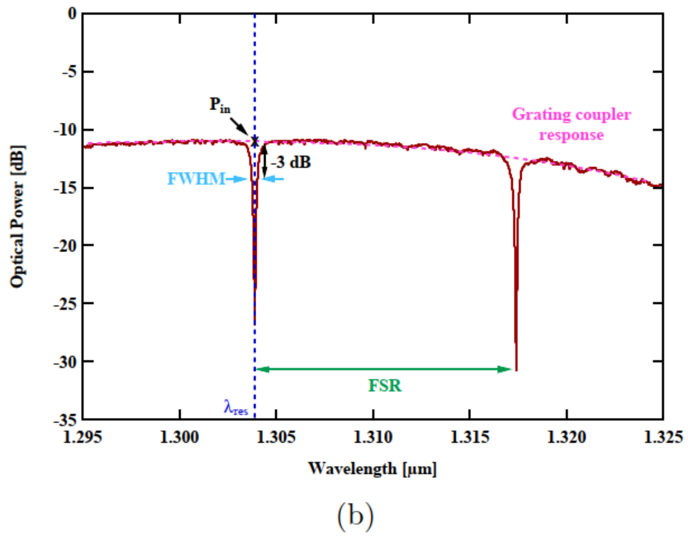

Figure 4: (a) All-pass configuration of the RM, with the coefficients of the electromagnetic fields. (b) Optical spectrum at the output, with the characteristic resonance profiles.

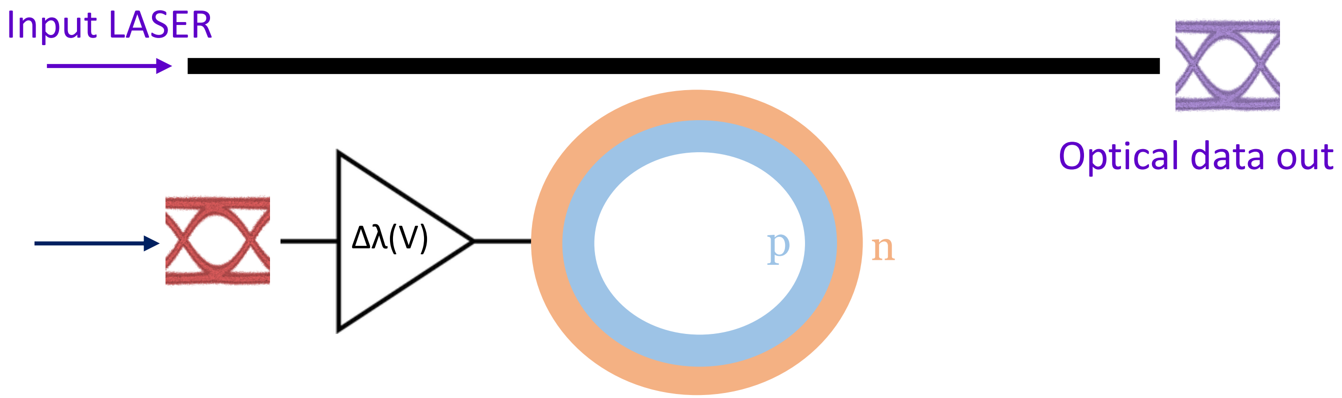

Introduction – Optical coupling

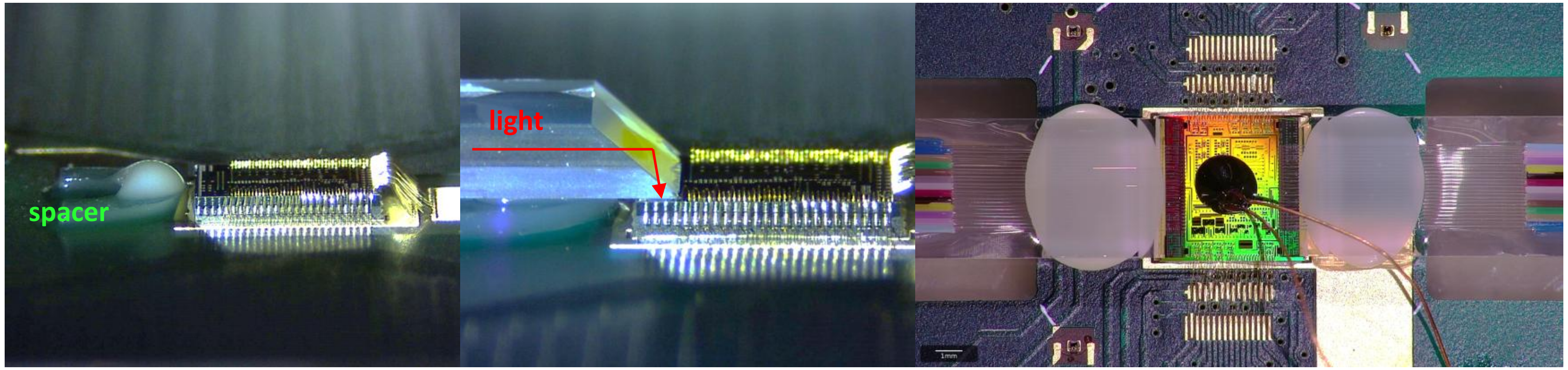

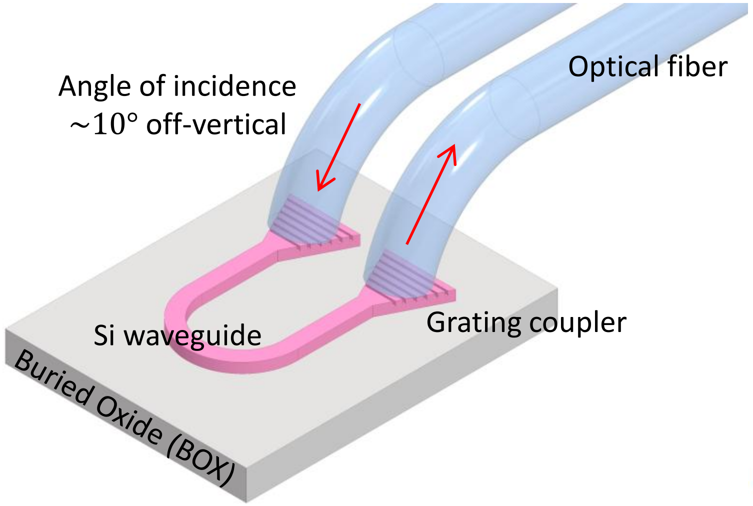

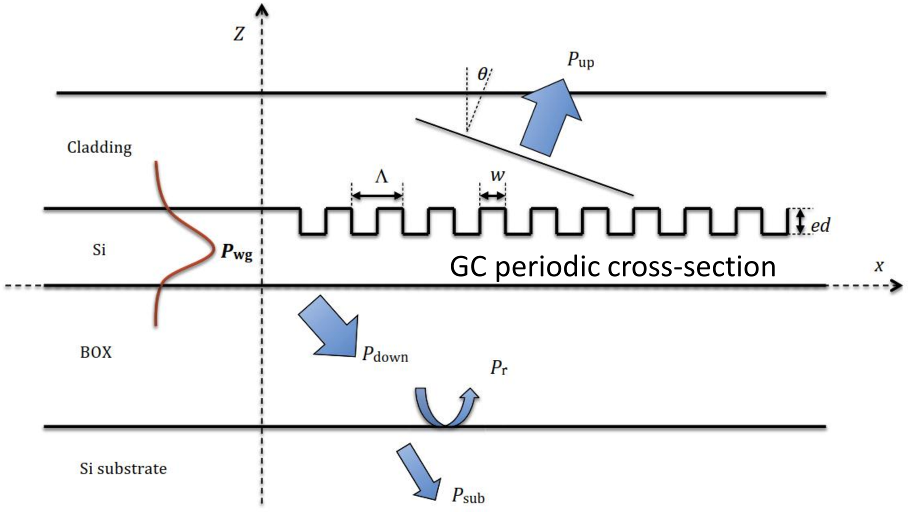

Figure 5.1 Schematic cross-section diagram of a grating coupler.

*https://doi.org/10.1017/CBO9781316084168.006

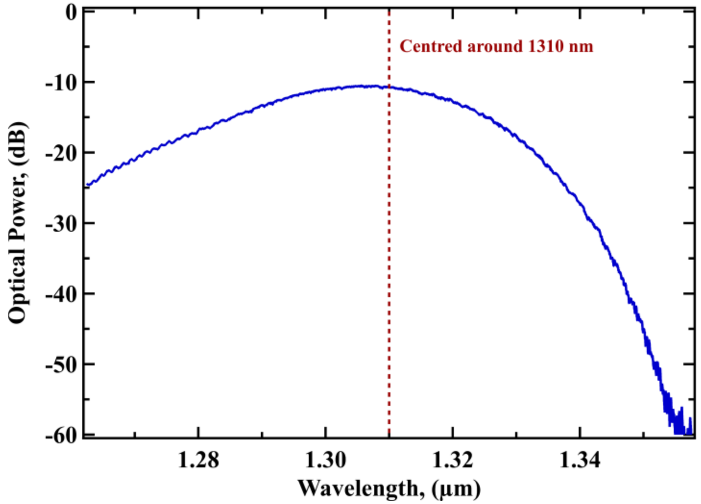

Static X-ray Test Setup

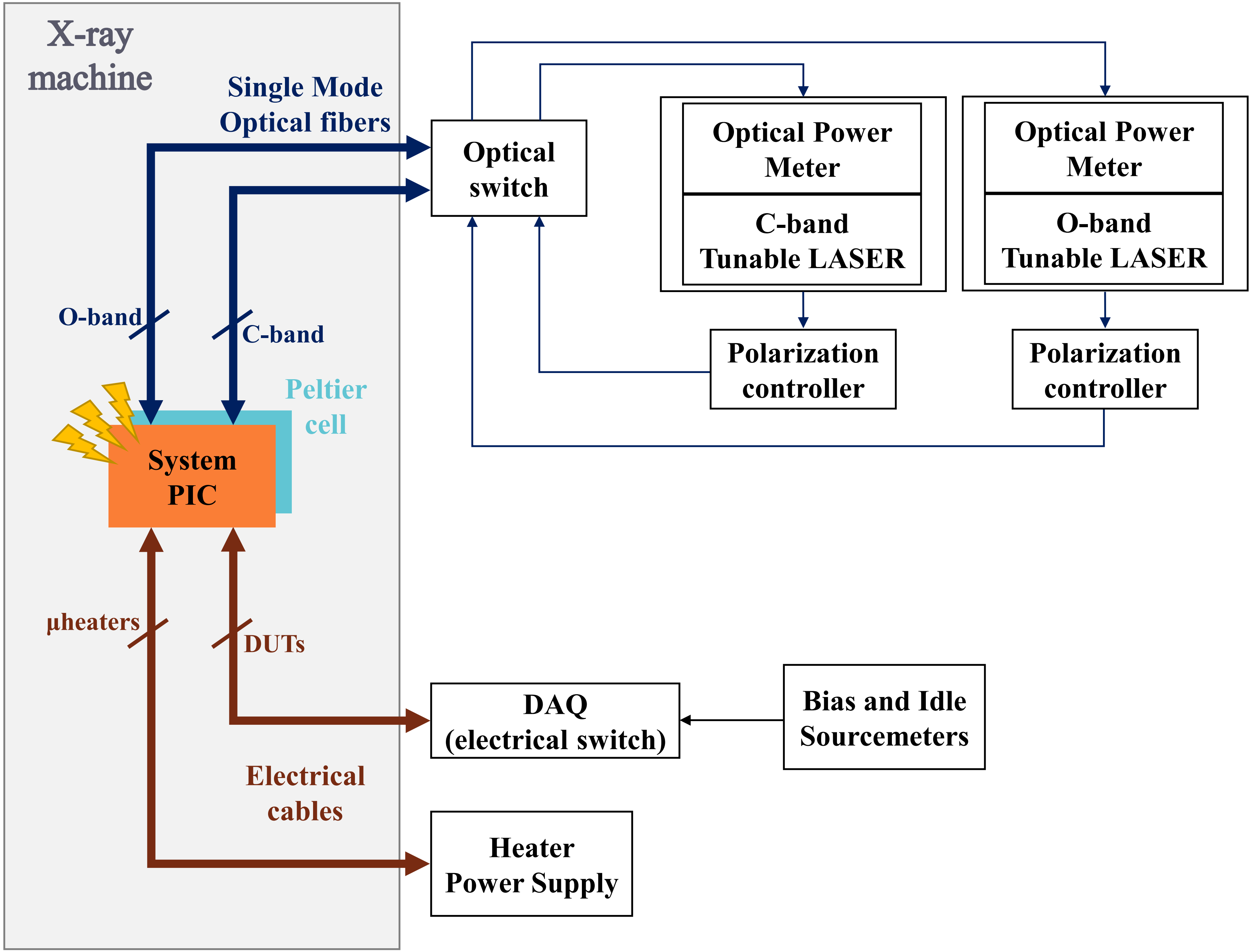

Static X-ray Test – Setup

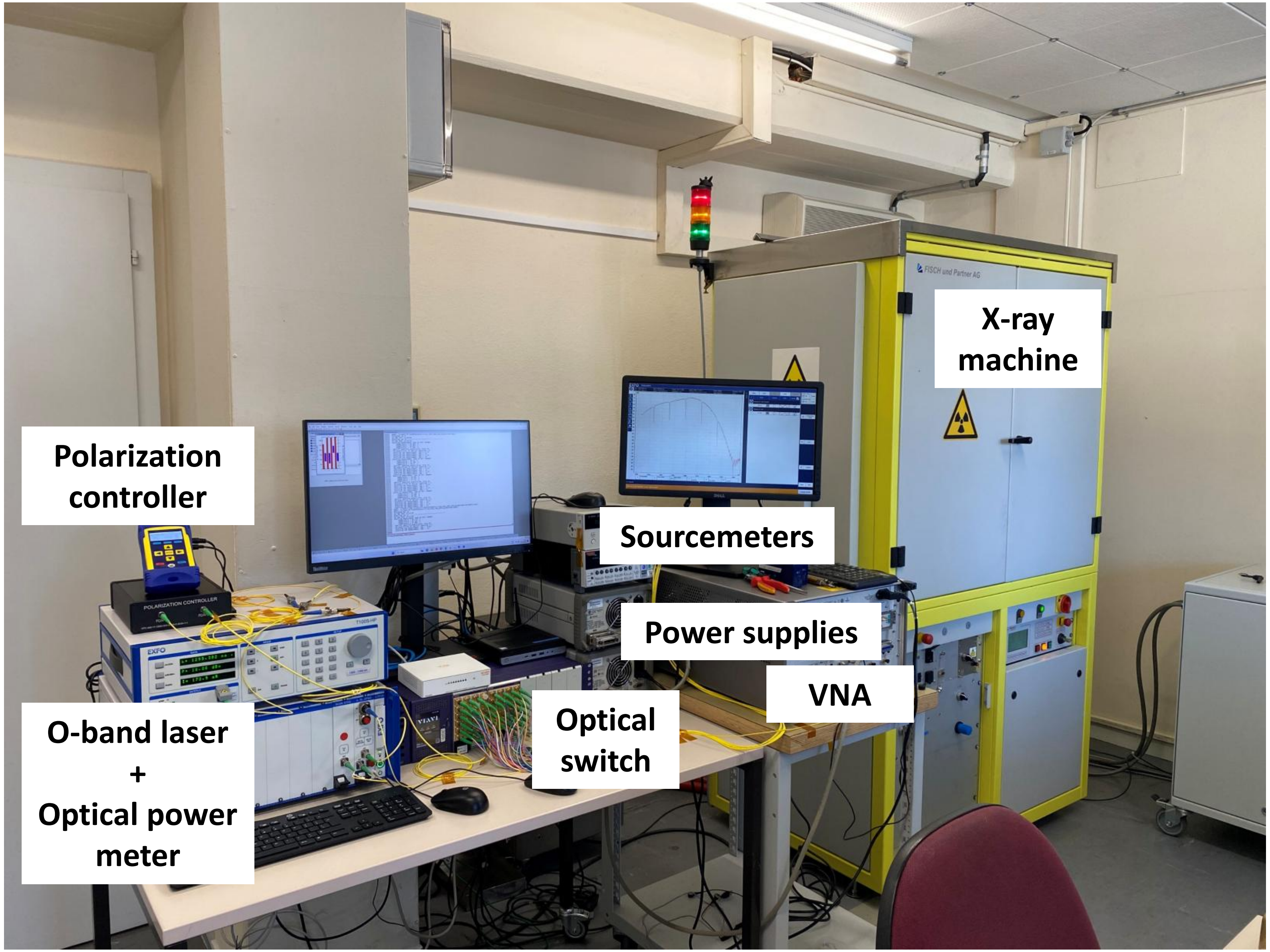

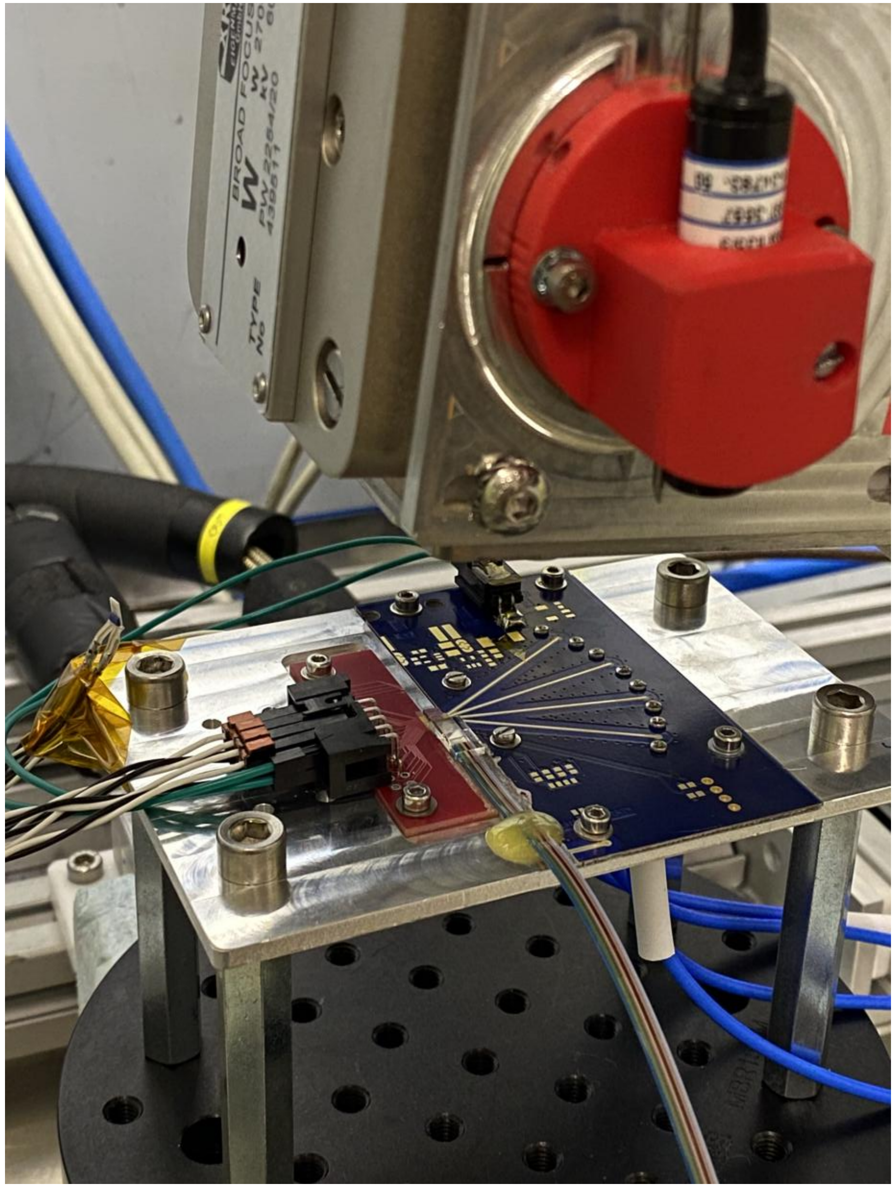

Static X-ray Test – IVs pre-irrad

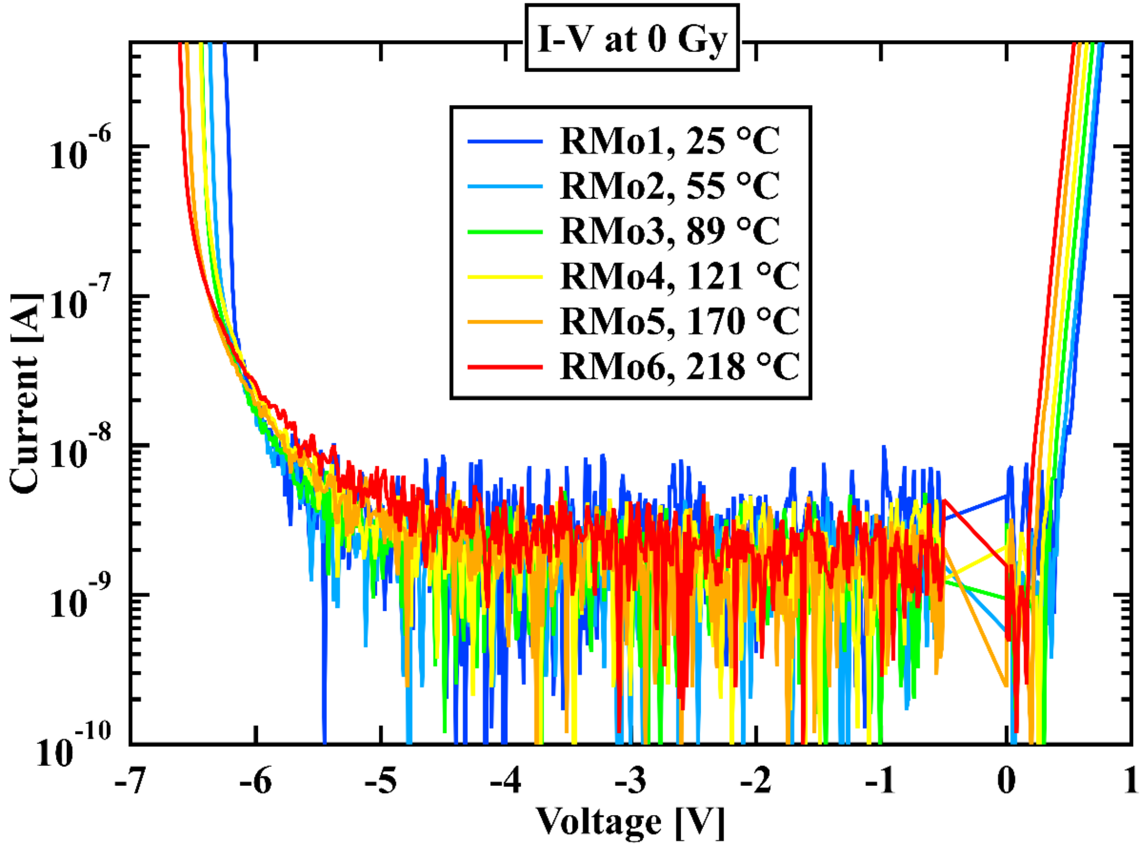

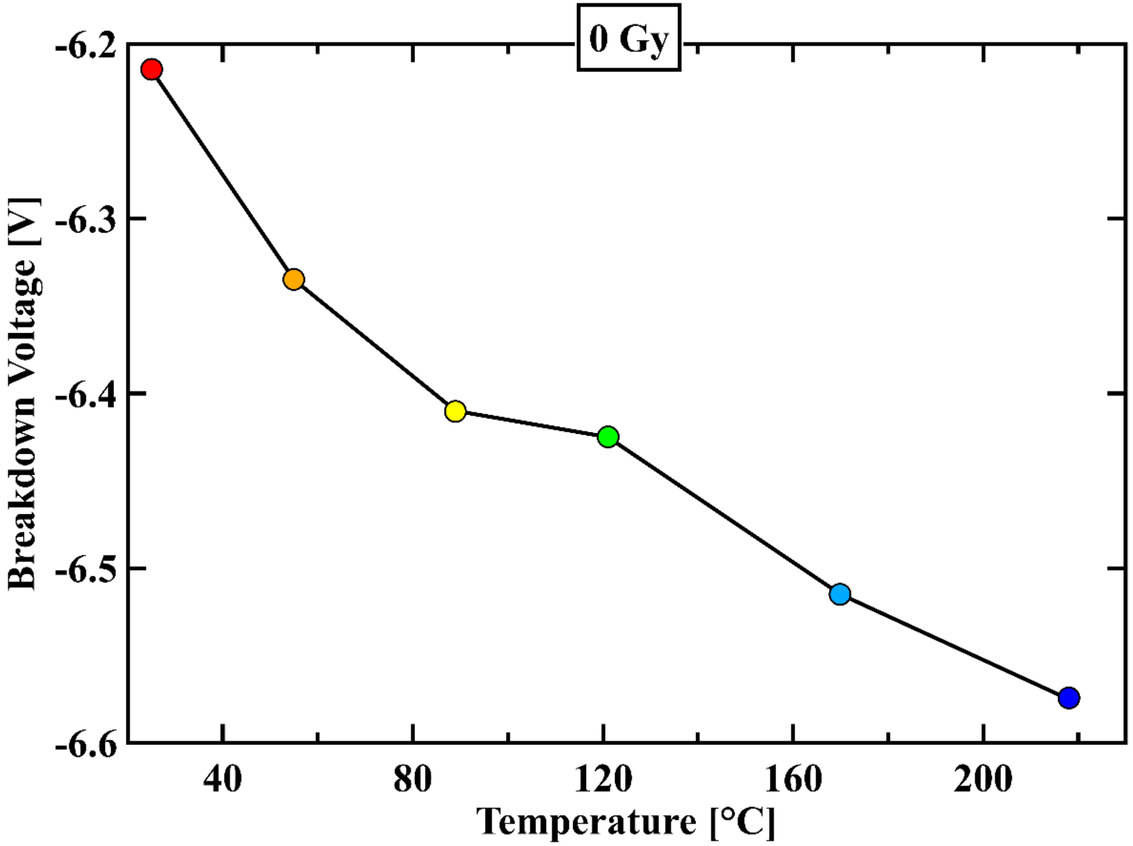

Dynamic X-ray Test Setup

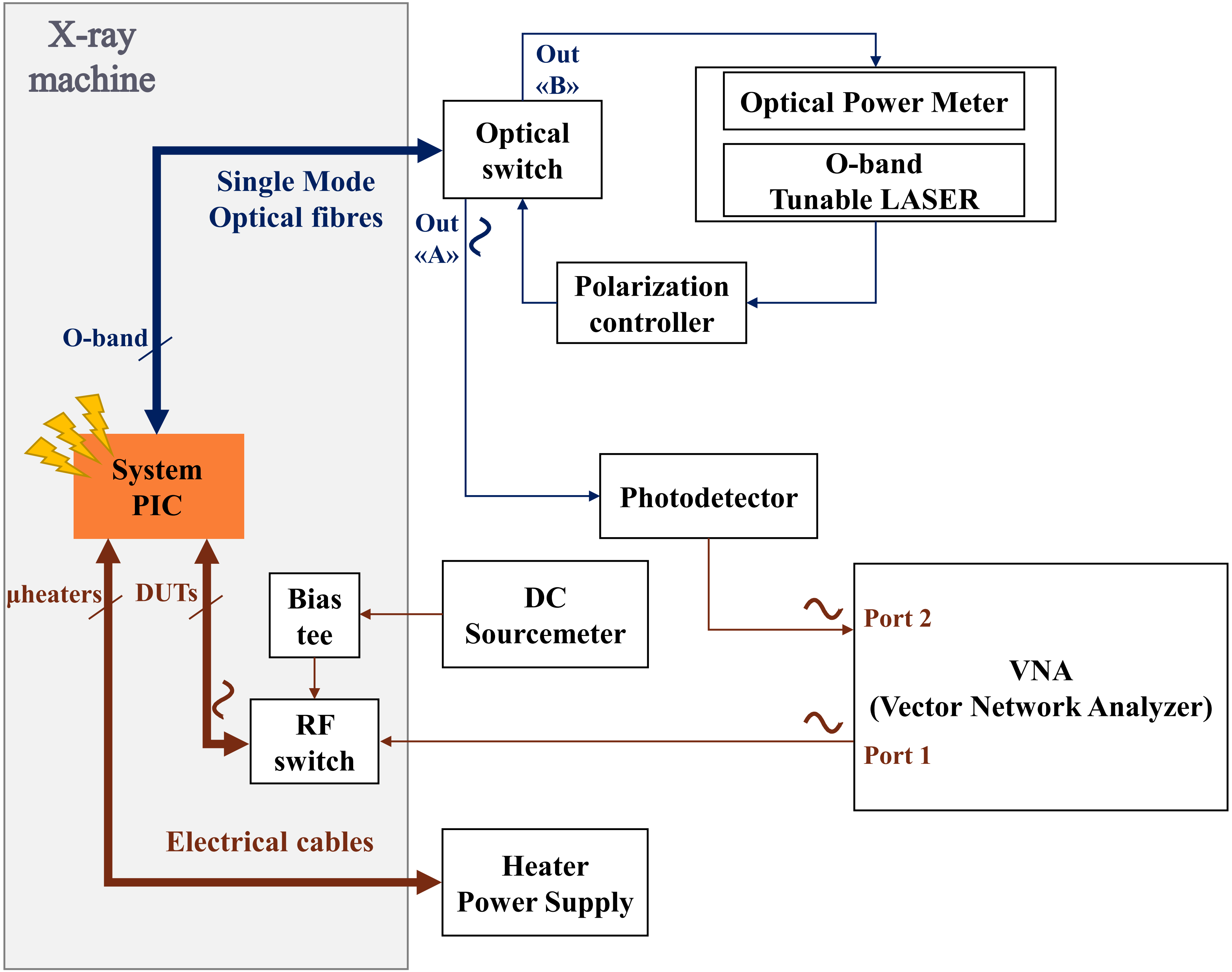

Dynamic X-ray Test – Setup

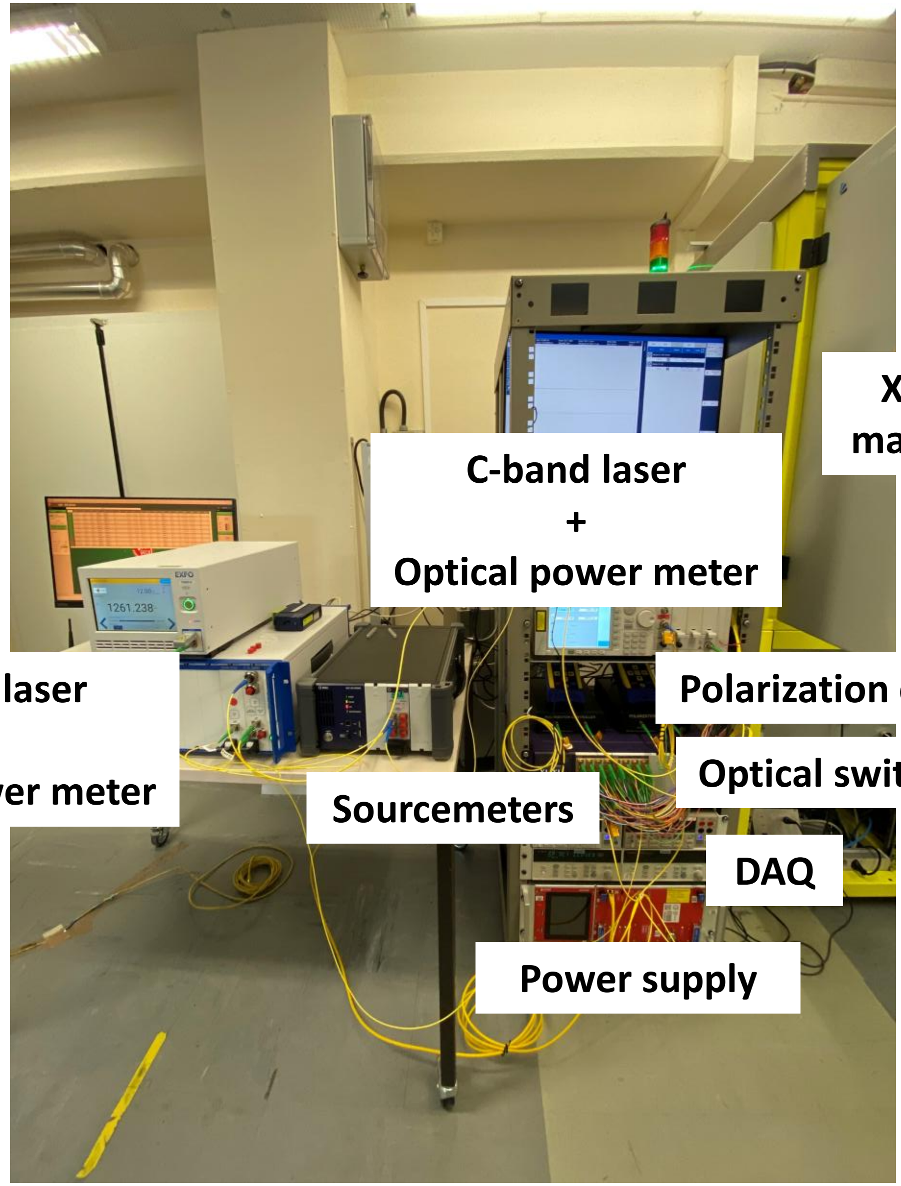

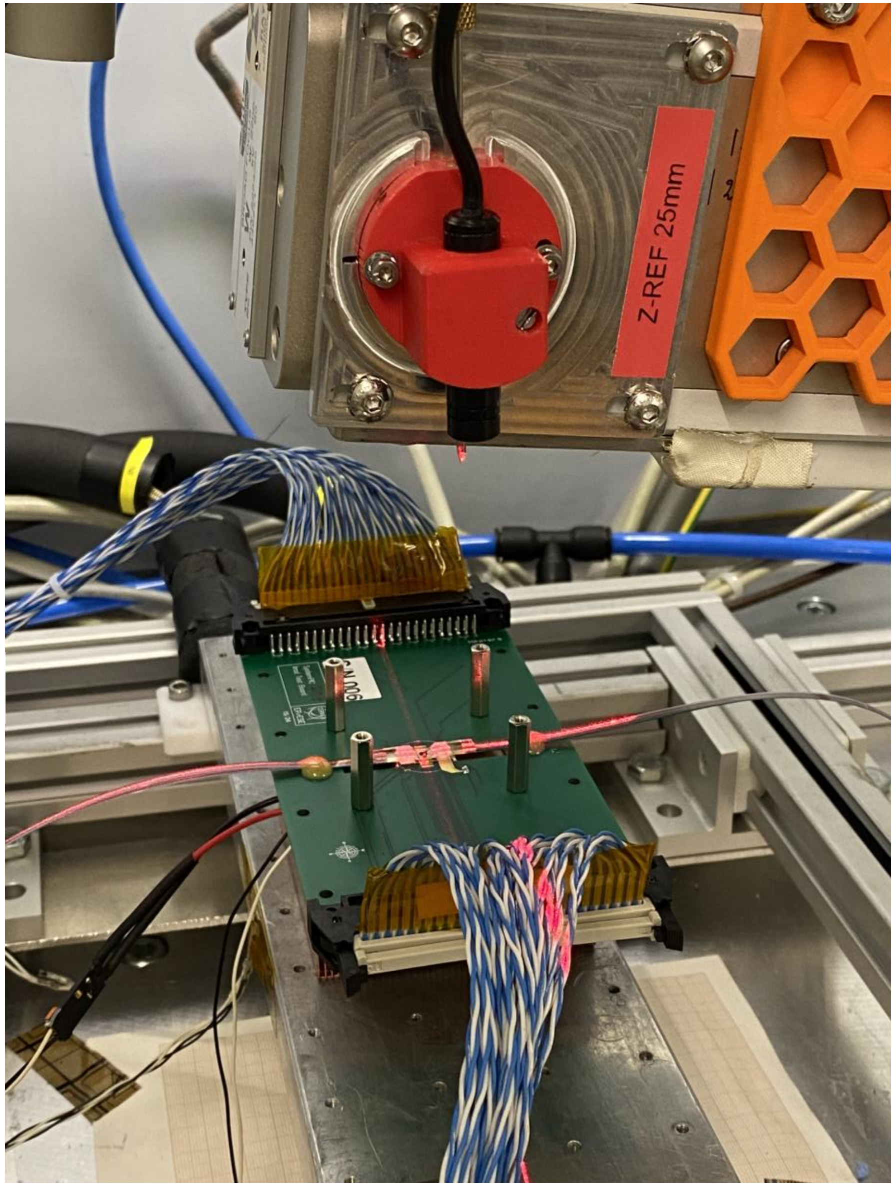

Dynamic X-ray test – RM efficiency

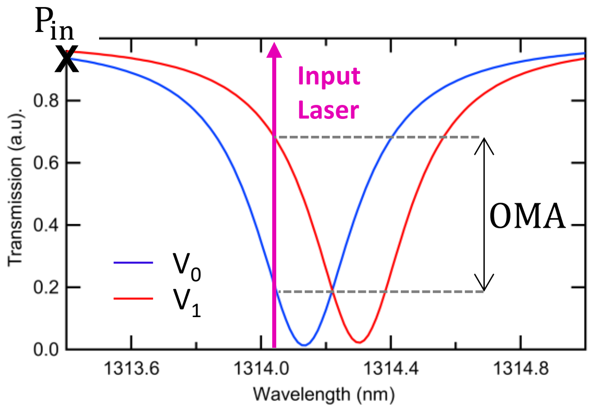

RM efficiency, defined as:

$$\eta(V_{mod}) = \frac{OMA}{P_{in}},$$

of the irradiated sample **did not change after exposure to 12.3 MGy**, following the annealing procedure

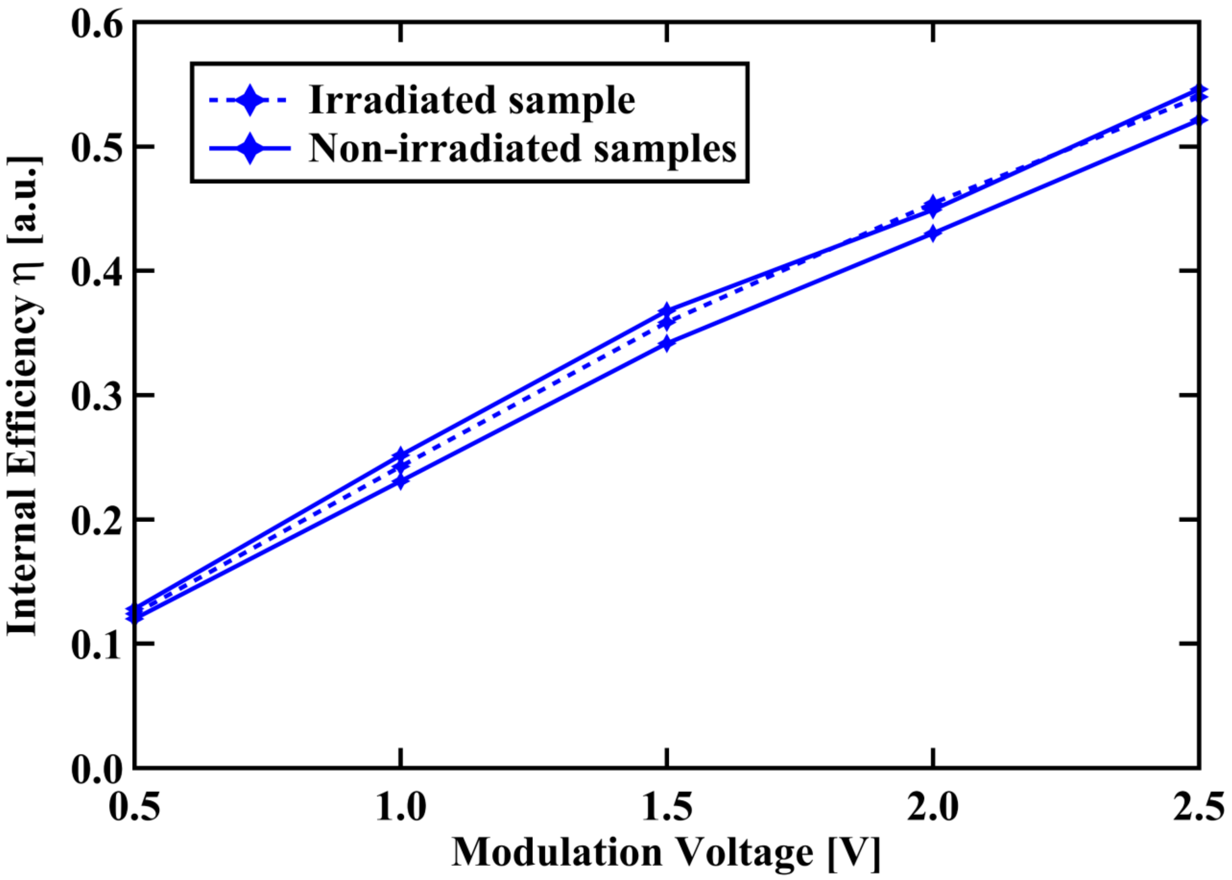

Neutron test – Setup

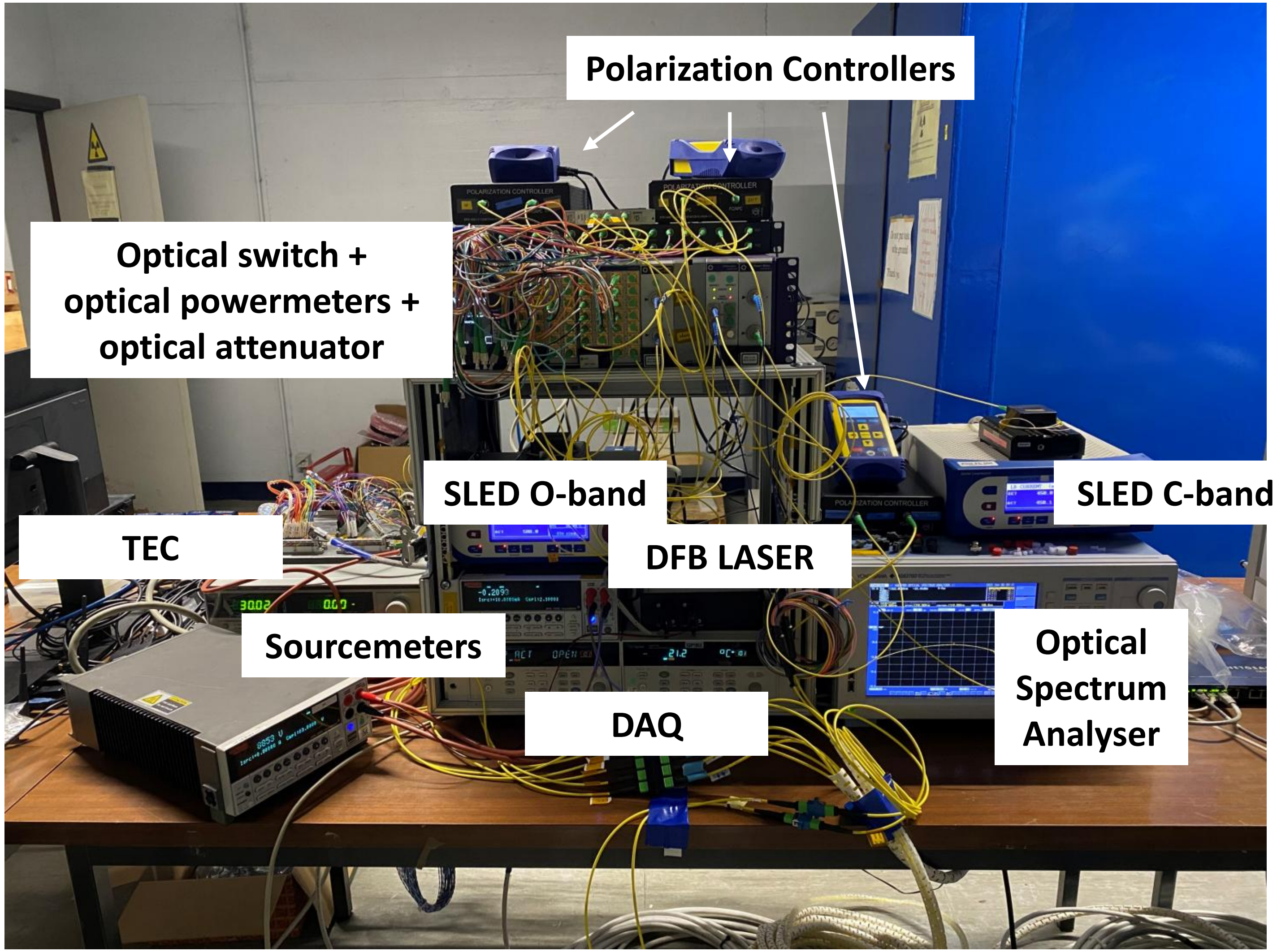

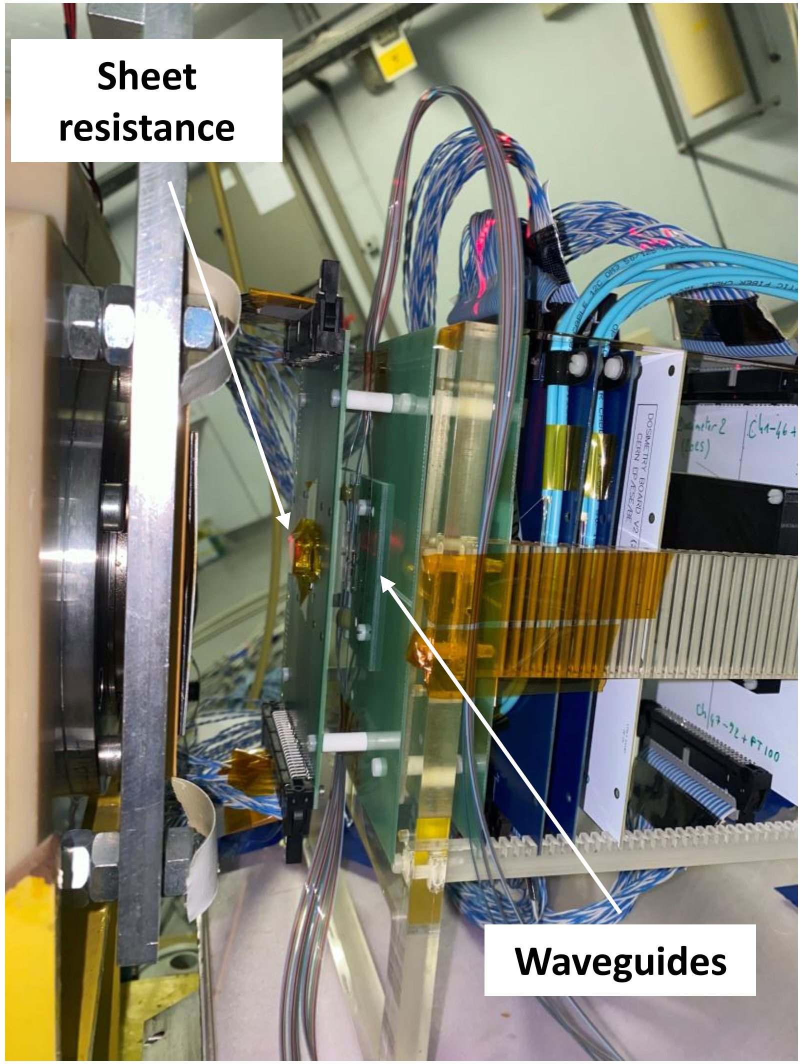

Beam distance: 4.5 cm for sheet resistance - 6.05 cm for cSKT, cWG, oSKT, oWG – 6.65 cm for cFC, oFC, Nonlinearity

Neutron test – Explaining the results

$q \rightarrow y - intercept \rightarrow grating\ coupler$

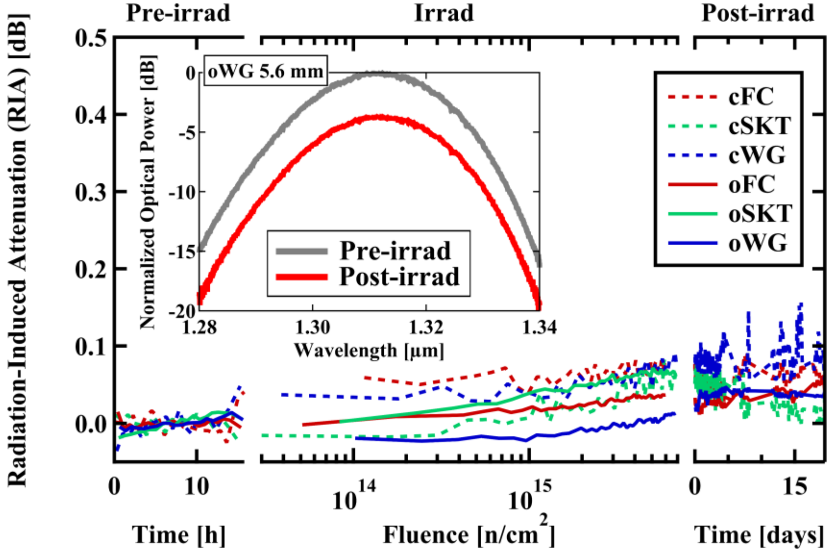

Analogous phenomena are observed in other applications, such as defect-based photon emitters for quantum computing, where several defect complexes exhibit emission in the O-band. In particular, T-, I-, and G-centers all show emission at photon energies around 0.95 eV [24]. These defects, commonly referred to as color centers, are typically generated in silicon through carefully controlled temperature and irradiation procedures, and they are used as emitters around cryogenic temperatures. While their formation in clusters due to high-energy neutron irradiation has not been directly demonstrated, it could plausibly contribute to increased absorption around 1.31 µm, especially considering the lack of silicon-based emitters in the C-band [25]. Identifying the specific mechanisms responsible for this absorption is beyond the scope of the present work, but future studies could provide further insight into the wavelength-dependent effects of neutron-induced defects in SiPh structures.

$y = mx + q$

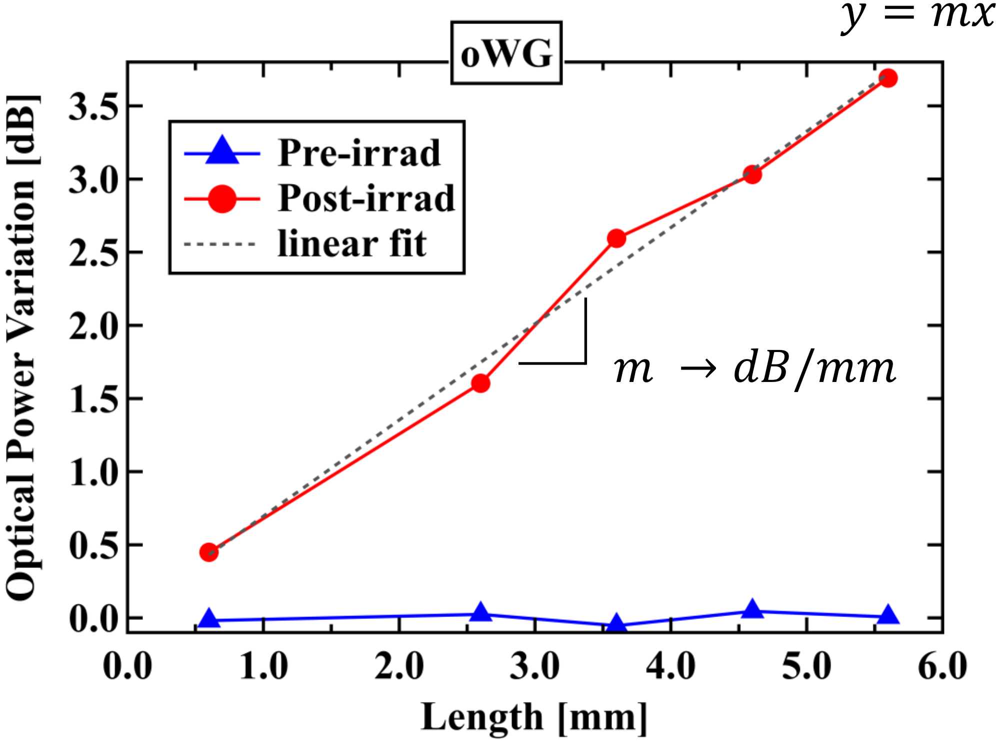

$m \rightarrow dB/mm$

[24] P. P. Filippatos, A. Chroneos, and C. A. Londos, "Re-examination of important defect complexes in silicon: From microelectronics to quantum computing," *Journal of Applied Physics*, vol. 137, no. 23, p. 230701, 06 2025. [Online]. Available: https://doi.org/10.1063/5.0276550
[25] G. Andrini, F. Amanti, F. Armani, V. Bellani, V. Bonaiuto, S. Cammarata *et al.*, "Solid-state color centers for single-photon generation," *Photonics*, vol. 11, no. 2, 2024. [Online]. Available: https://www.mdpi.com/2304-6732/11/2/188

Neutron test – oWG annealing

If we plot the increase in linear loss together with the RIA coefficient for the oWG waveguides, the discrepancy between the two measurements becomes evident.

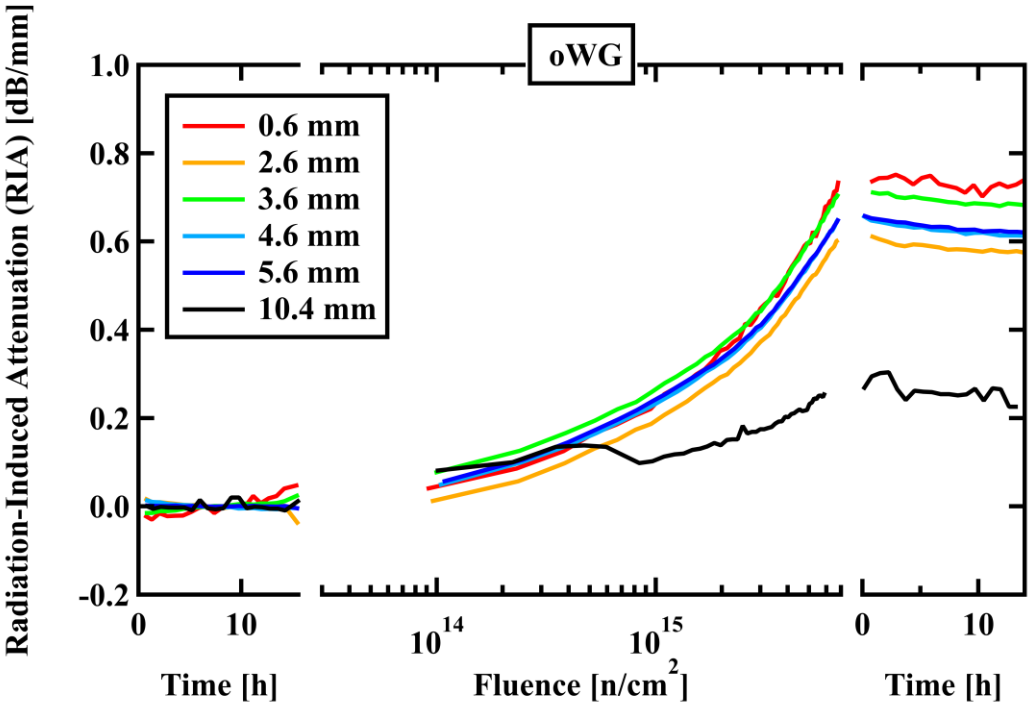

The RIA coefficient, calculated from the increase in linear loss for the 10.4 mm sample, shows a much smaller increase with neutron fluence compared to the other waveguides. This is likely due to a photobleaching effect that induces partial annealing in the waveguide when high optical power is injected. This observation should be emphasized in a potential publication, as it is both important for understanding the behaviour of the device. However, at the same time, this is promising for our application, since it indicates that the calculated RIA coefficient is likely an overestimation.

N.B. For a mistake in the acquisition loop, I forgot to set the attenuation to 25dB in the idle time, that's why we have this annealing effect. The power into the waveguide during the test was $\sim 14.9\ mW$ (calculated from P_0). Even if this was a mistake, it actually gives us an extra data point which is really useful.

X-ray test – GC variation

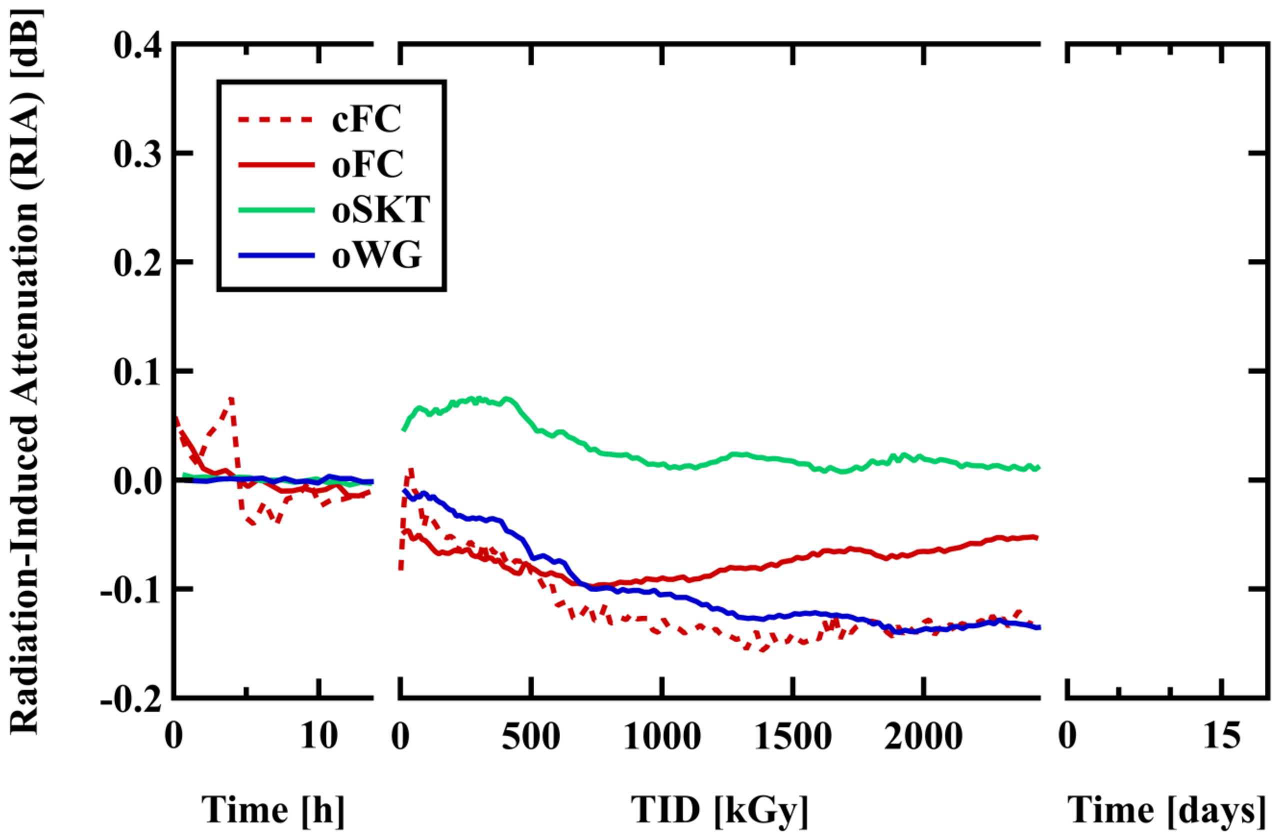

Heavy ion test – Setup

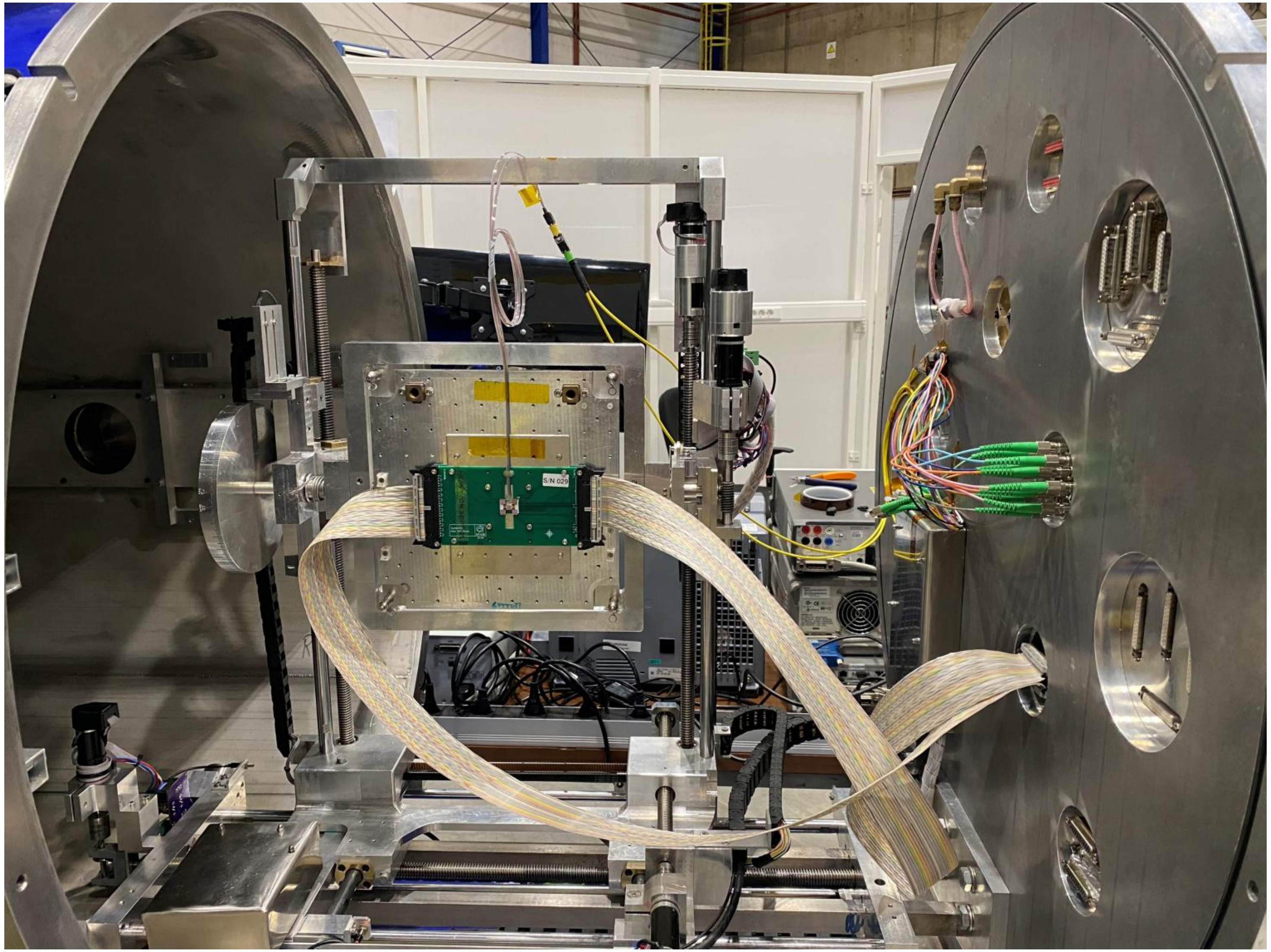

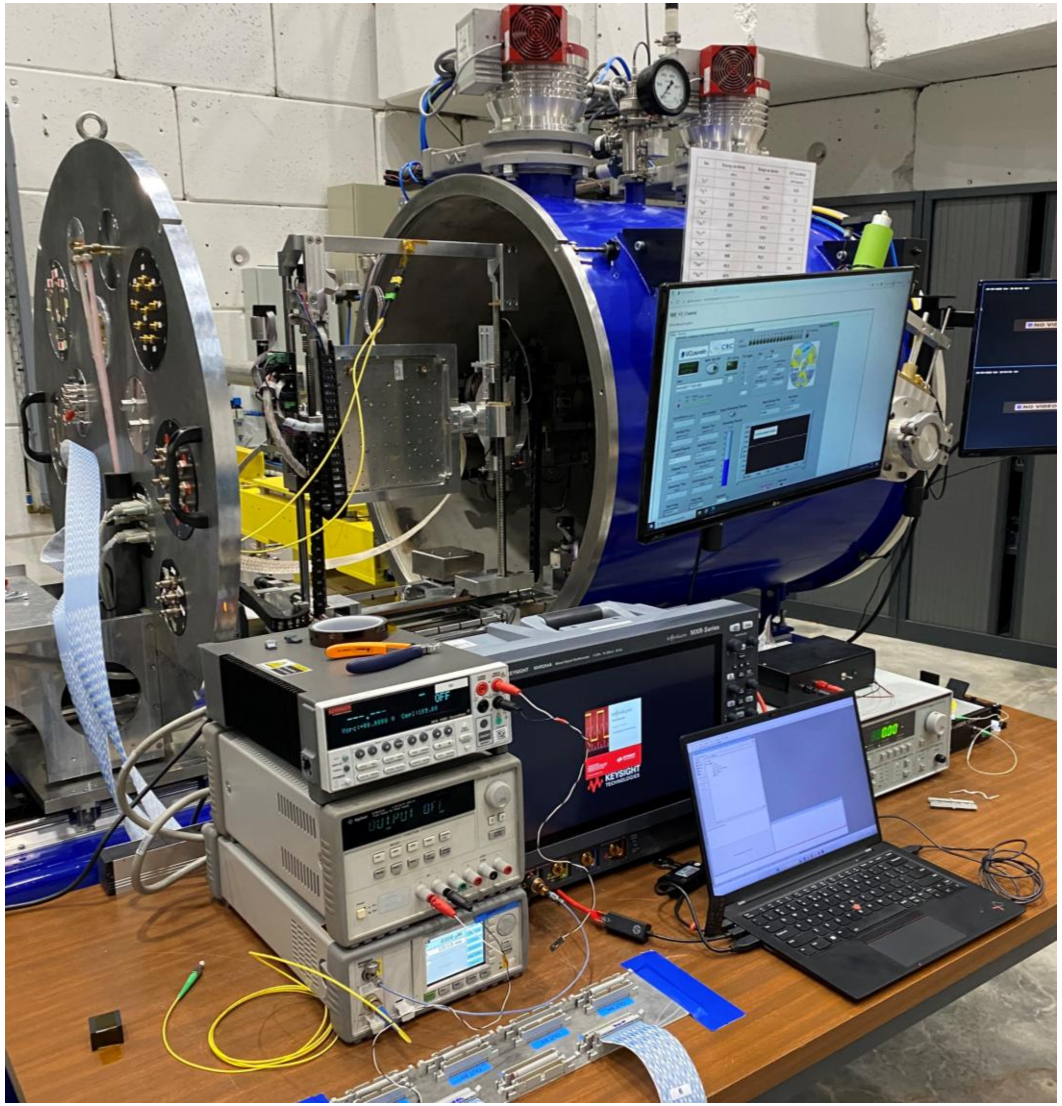

Heavy ion test – TCAD simulation

TCAD mesh

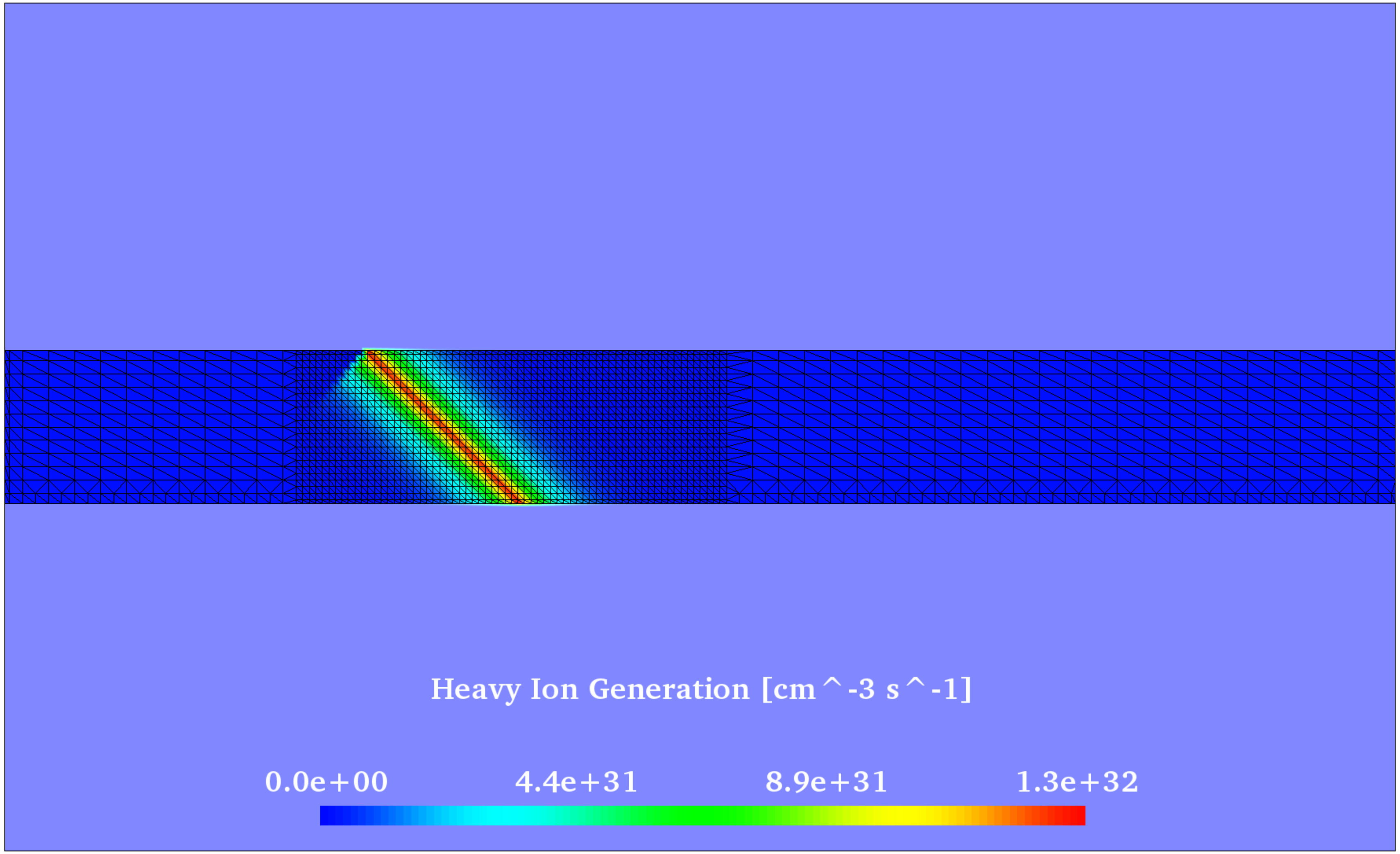

We have to imagine that $N(r)$ is a 2D exponential function which describes the carrier generation along the ion propagation. The carrier generated are considered uniform along the penetration direction:

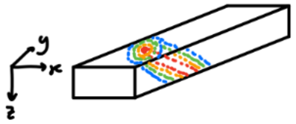

We can consider one plane along z. The carrier generated are:

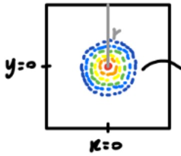

$$N(r) = N_0 \cdot e^{-r/\sigma_{ion}} \quad \text{where} \quad N_0 = N(x=0, y=0)$$

Therefore, for each coordinate point the radius can be described as:

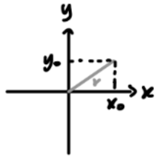

$$r = \sqrt{x_0^2 + y_0^2}$$

By building a mesh grid on MATLAB, the 2D carrier density is given by:

$$N(x,y) = N_0 \cdot e^{-\sqrt{x_0^2+y_0^2}/\sigma_{ion}}$$

To get (8), I need to take the radial section using cylindrical coordinates:

$$\iint N(x,y)\,dx\,dy \quad ; \quad r = \sqrt{x^2+y^2} \quad ; \quad x = r\cdot\cos\theta \quad ; \quad y = r\cdot\sin\theta$$

we need to change the coordinates by calculating the Jacobian:

$$dx\,dy = |J|\,dr\,d\theta$$

$$J = \begin{vmatrix} \partial x/\partial r & \partial x/\partial\theta \\ \partial y/\partial r & \partial y/\partial\theta \end{vmatrix} = \begin{vmatrix} \cos\theta & -r\sin\theta \\ \sin\theta & r\cos\theta \end{vmatrix} = (\cos\theta\cdot r\cos\theta) - (-r\sin\theta\cdot\sin\theta) = r\cos^2\theta + r\sin^2\theta = r$$

$$\Rightarrow dx\,dy = r\,dr\,d\theta = dA$$

The integral becomes:

$$\iint N(x,y)\,dx\,dy = \int_S N(r)\,dA = \int_0^{2\pi}\int_0^{+\infty} N(r)\cdot r\,dr\,d\theta,$$

since $N(r)$ does not depend on $\theta \Rightarrow \int_0^{2\pi} d\theta = 2\pi$

$$\Rightarrow 2\pi\int_0^{+\infty} r\cdot N(r)\,dr = 2\pi N_0 \int_0^{+\infty} r\cdot e^{-r/\sigma_{ion}}\,dr$$

* $t = \dfrac{r}{\sigma_{ion}} \Rightarrow r = t\cdot\sigma_{ion} \Rightarrow dr = \sigma_{ion}\,dt$, for $r\to+\infty$ also $t\to+\infty$ *

$$\Rightarrow 2\pi N_0 \int_0^{+\infty} t\cdot\sigma_{ion}\, e^{-t}\cdot\sigma_{ion}\,dt = 2\pi N_0\sigma_{ion}^2 \int_0^{+\infty} t\cdot e^{-t}\,dt$$

* $\int f\cdot g' = f\cdot g - \int f'\cdot g \Rightarrow f = t$ and $g' = e^{-t}$

$$\Rightarrow \int t\cdot e^{-t}\,dt = t(-e^{-t}) - \int -e^{-t}\,dt = -t\cdot e^{-t} + \int e^{-t}\,dt$$ *

$$\Rightarrow 2\pi N_0\sigma_{ion}^2 \int_0^{+\infty} t\cdot e^{-t}\,dt = 2\pi N_0\sigma_{ion}^2\left[-t\cdot e^{-t} - e^{-t}\right]_0^{+\infty} = 2\pi N_0\sigma_{ion}^2\left[-(t+1)e^{-t}\right]_0^{+\infty}$$

* $\lim_{t\to+\infty} -(t+1)\cdot e^{-t} \to 0$ exponential has higher order of infinity than polynomial

$\lim_{t\to 0} -(t+1)\,e^{-t} \to -1$ *

$$\Rightarrow 2\pi N_0\sigma_{ion}^2\left[0-(-1)\right] = 2\pi N_0\sigma_{ion}^2 \quad \Rightarrow \quad \iint N(x,y)\,dx\,dy = 2\pi N_0\sigma_{ion}^2$$

Heavy ion test – TCAD simulation

$$\frac{LET \cdot \rho_{Si}}{\varepsilon_{ehp}} = \frac{eV \cdot m^2}{g} \cdot \frac{g}{m^3} \cdot \frac{pair}{eV} = \left[\frac{pair}{m}\right]$$ i.e. the pairs generated per unit of length

This number can be converted in charge linear density:

$$\frac{LET \cdot \rho_{Si}}{\varepsilon_{ehp}} = 2\pi N_0 \sigma_{ion}^2 = \frac{Q_0}{h}$$, where Q_0 is the total number of ehp generated

You can see it starting from the result of the integral:

$$\int_0^{+\infty} N(r)\,dr = 2\pi N_0 \sigma_{ion}^2 \quad [ehp/m]$$ ⇒ we calculated the # of ehp created radially, per unit of surface, along the ion track

Therefore, if we multiply our result for the height of the waveguide (in case of vertical incidence), we get the volumetric number of ehp generated (if the radial density is considered constant):

$$Q_0 = h \cdot (2\pi N_0 \sigma_{ion}^2) \Rightarrow 2\pi N_0 \sigma_{ion}^2 = \frac{Q_0}{h}$$

- $N(r) = N_0 e^{-r/\sigma_{ion}}$
- $\frac{LET \cdot \rho_{Si}}{\varepsilon_{ehp}} = 2\pi N_0 \sigma_{ion}^2 = \frac{Q_0}{h}$
- $\frac{LET \cdot \rho_{Si}}{\varepsilon_{ehp}} = 3.9455 \times 10^{10}\, ehp/cm$
- $h = 220\, nm \rightarrow Q_0 \approx 868021\, ehp$
- $\rightarrow N_0 = \frac{Q_0}{2\pi h \sigma_{ion}^2}$

For a defined value of σ_{ion}^2 we can find the corresponding N_0:

- $\sigma_{ion} = 10\, nm \rightarrow N_0 \approx 6.28 \times 10^{21}\, ehp/cm^3$
- $\sigma_{ion} = 20\, nm \rightarrow N_0 \approx 1.57 \times 10^{21}\, ehp/cm^3$
- $\sigma_{ion} = 30\, nm \rightarrow N_0 \approx 6.98 \times 10^{20}\, ehp/cm^3$ → Selected $\sigma_{ion} = 30\, nm$ for all simulations

Heavy ion test – TCAD simulations

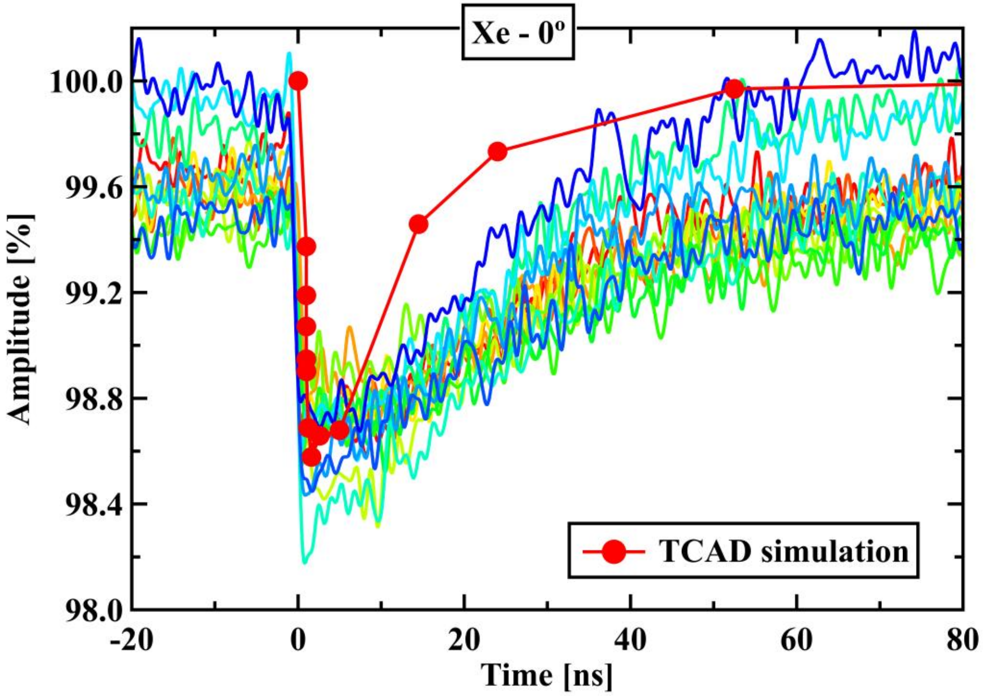

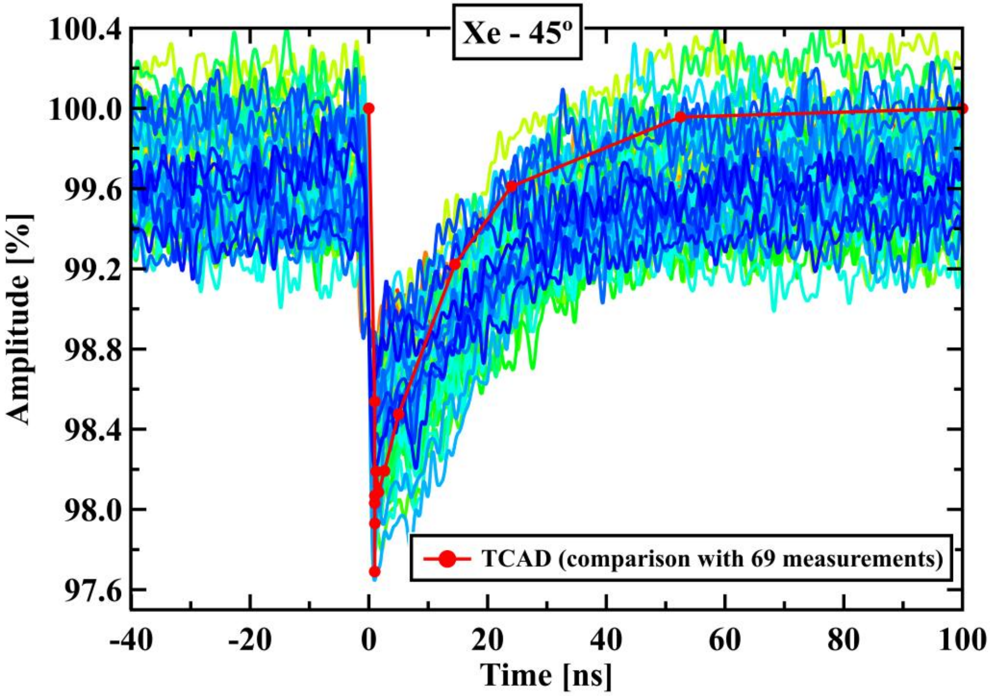

Heavy ion test – Recombination mechanisms